



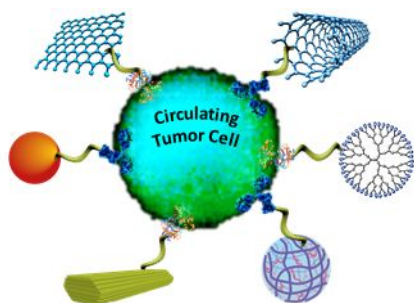
## Chemo-specific Designs for the Enumeration of Circulating Tumor Cells: Advances in Liquid Biopsy

Journal:	<i>Journal of Materials Chemistry B</i>
Manuscript ID	TB-REV-11-2020-002574.R1
Article Type:	Review Article
Date Submitted by the Author:	09-Dec-2020
Complete List of Authors:	<p>Singh, Balram; Actorius Innovations and Research            Arora, Smriti; Actorius Innovations and Research , Research            D'Souza, Alain; Actorius Innovations and Research ,            Kale, Narendra; Actorius Innovations and Research            Aland, Gourishankar ; Actorius Innovations and Research            Bharde, Atul; Savitribai Phule Pune University, Department of            Microbiology            Quadir, Mohiuddin; North Dakota State University, Coatings and            Polymeric Materials; North Dakota State University, Coatings and            Polymeric Materials            Calderon, Marcelo; POLYMAT, Basque Center for Macromolecular Design            and Engineering,            Chaturvedi, Pankaj; Tata Memorial Hospital, Surgical Oncology            Khandare, Jayant; School of Pharmacy, Dr. Vishwanath Karad            Maharashtra Institute of Technology-World Peace University</p>

## Chemo-specific Designs for the Enumeration of Circulating Tumor Cells: Advances in Liquid Biopsy

Balram Singh<sup>†b</sup>, Smriti Arora<sup>†b</sup>, Alain D'Souza<sup>b</sup>, Narendra Kale<sup>b</sup>, Gourishankar Aland<sup>b</sup>, Atul Bharde<sup>b,c</sup>, Mohiuddin Quadir<sup>d</sup>, Marcelo Calderón<sup>e,f</sup>, Pankaj Chaturvedi<sup>g</sup>, Jayant Khandare<sup>a,b\*</sup>

**Chemical platforms for isolation and enumeration of Circulating Tumor Cells (CTCs) in advancing relevance of liquid biopsy in cancer diagnostics and treatment.**



## ARTICLE

## Chemo-specific Designs for the Enumeration of Circulating Tumor Cells: Advances in Liquid Biopsy

Received 00th January 20xx,  
Accepted 00th January 20xx

Balram Singh<sup>†b</sup>, Smriti Arora<sup>†b</sup>, Alain D'Souza<sup>b</sup>, Narendra Kale<sup>b</sup>, Gourishankar Aland<sup>b</sup>, Atul Bharde<sup>b,d</sup>, Mohiuddin Quadir<sup>e</sup>, Marcelo Calderón<sup>f,g</sup>, Pankaj Chaturvedi<sup>h</sup>, Jayant Khandare<sup>a,b,c\*</sup>

DOI: 10.1039/x0xx00000x

Advanced materials and chemo-specific designs at the nano/micrometer-scale have ensured revolutionary progress in next-generation clinically relevant technologies. For example, isolating a rare population of cells, like circulating tumor cells (CTCs) from the blood amongst billion of other blood cells, is one of the most complex scientific challenges in cancer diagnostics. The chemical tunability to achieve this degree of exceptional specificity for extra-cellular biomarker interactions demands the utility of advanced entities and multistep reactions both in solution and insoluble state. Thus, this review delineates the chemo-specific substrates, chemical methods, and structure-activity relationship (SAR) of chemical platforms used for isolation and enumeration of CTCs in advancing the relevance of liquid biopsy in cancer diagnostics and disease management. We highlight the synthesis of cell-specific, tumor biomarker-based, chemo-specific substrates utilizing functionalized linkers through chemistry-based conjugation strategies. These nano/micro substrates' capacity to enhance the cell interaction specificity and efficiency with the targeted tumor cells is detailed. Furthermore, this review accounts for the importance of CTC capture and other downstream processes involving genotypic and phenotypic CTC analysis in real-time for detection of early onset of metastases progression, chemotherapy treatment response, and in monitoring progression free-survival (PFS), disease-free survival (DFS), and eventually overall survival (OS) in cancer patients.

### 1. Introduction

Various advanced materials have been proposed for biological and clinical applications in theranostics, imaging, and diagnostics.<sup>1-10</sup> The synthetic strategies in designing such advanced materials involve the prodigious combination of coordination, conjugation, and bioorthogonal reactions; hybridizing both chemical and biological entities or substrates, such as carbon allotropes, linear and hyperbranched polymers, iron oxide nanoparticles (FeNPs), silver nanoparticles (AgNPs), gold nanoparticles (AuNPs), silicates, proteins, antibodies, etc. (**Figure 1**).<sup>1-4, 9</sup> The synthetic strategies adopted to design such materials impart the desired structure-activity relationships (SAR), and enable control over the physicochemical traits including, architecture, micro/nano size, surface charge,

branching, spatial control, stimuli sensitivity, medium dispersibility, etc.<sup>11-17</sup> Thus, the capacity to control the attributes mentioned above have improved the specificity and efficiency for various biological applications including infectious diseases, blood disorders, and detection of cancer both at phenotype and genotype levels.<sup>18-20</sup>

Metabolic disorders in developing countries and cancer incidences in developed countries have been rising at an alarming rate. In particular, cancer is responsible for one in six deaths, the second most common cause of mortality globally.<sup>21</sup> Thus, cancer disease management stresses a multidisciplinary scientific approach involving cellular, proteomic, and genomic-based diagnostic capacities combined into a single platform due to tumor heterogeneity and longitudinal information of the disease. Such a platform will improve clinical disease status determination, and in addition, act as an enabling technology for treatment monitoring, responses, and outcomes.<sup>21</sup> Furthermore, the disease burden has been enhanced socio-economically. This is further propelled by rapid population growth, ageing societies, lifestyles, and increasing commercial interests.<sup>22, 23</sup> In 2018, 18.1 million cancer incidences and 9.6 million cancer-related deaths were reported worldwide.<sup>22, 23</sup> Additionally, unhealthy lifestyles resulting from smoked or chewed tobacco use, alcohol abuse, and improper diet are propelling the prevalence of head and neck cancers globally, especially within Asian population where access to

<sup>a</sup> School of Pharmacy, Dr. Vishwanath Karad Maharashtra Institute of Technology-World Peace University, Kothrud, Pune 411038, India.

<sup>b</sup> Actorius Innovations and Research Pvt. Ltd., Pune, 411057 India.

<sup>c</sup> School of Consciousness, Dr. Vishwanath Karad Maharashtra Institute of Technology-World Peace University, Kothrud, Pune 411038, India.

<sup>d</sup> Current: Dept. of Microbiology, Savitribai Phule Pune University, Pune, 411007 India.

<sup>e</sup> Department of Coatings and Polymeric Materials, North Dakota State University, Fargo, ND, 58108, USA.

<sup>f</sup> POLYMAT and Applied Chemistry Department, Faculty of Chemistry, University of the Basque Country UPV/EHU, Paseo Manuel de Lardizabal 3, 20018 Donostia-San Sebastián, Spain.

<sup>g</sup> IKERBASQUE, Basque Foundation for Science, 48013 Bilbao, Spain.

<sup>h</sup> Department of Head and Neck Surgical Oncology, Tata Memorial Hospital, Mumbai, 400012 India.

<sup>†</sup> Authors contribute equally.

\*Corresponding author: jayant.khandare@mippune.edu.in, jayant@actorius.co.in

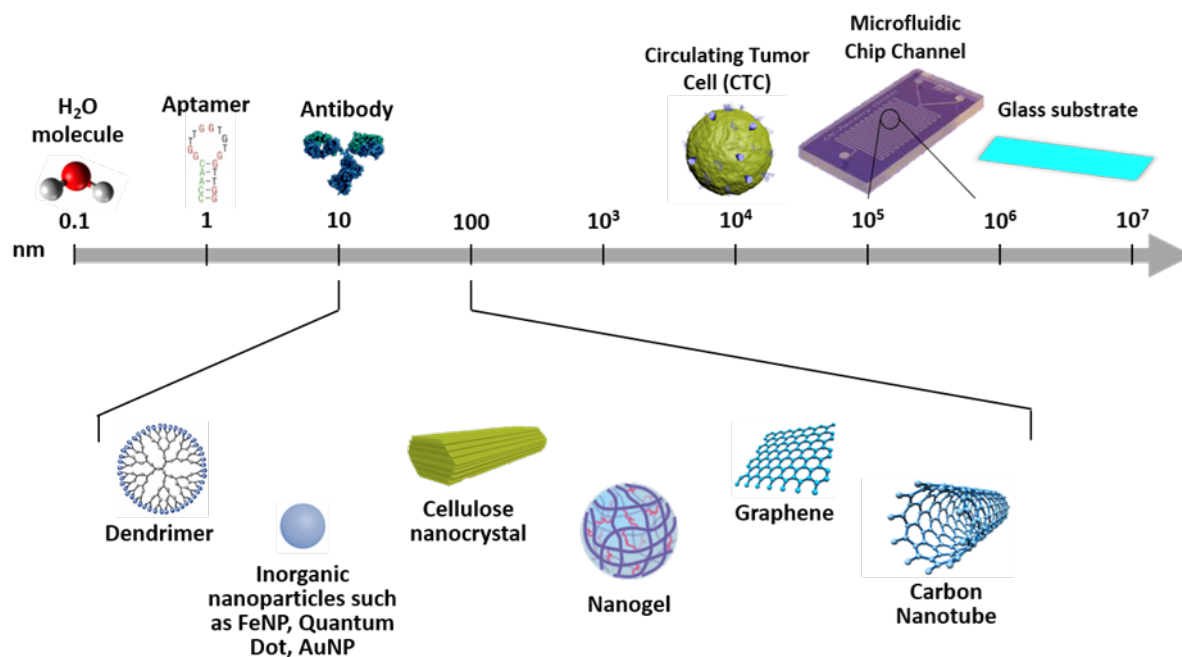


**Figure 1:** Length scale showing the size of nano/micro substrates compared to biochemical targeting ligands and circulating tumor cells (CTCs). The characteristic size of nano/micro- substrates places them in between the targeting ligands and CTCs.

advanced healthcare may not be readily available or affordable.<sup>24</sup> Unfortunately, 90% of cancer-related deaths are attributed to metastasis, and only 10% are related to primary tumorigenesis.<sup>25, 26</sup>

Metastasis involves extravasation and invasion of distant organ sites, triggered by CTCs through dissemination and intravasation from the site of a primary tumor, transport via the peripheral blood system, and colonization and formation of micro-metastatic sites at distant organs.<sup>27</sup> The significance of CTCs as an independent risk factor in several epithelial origin cancer types, termed carcinomas, has been identified in over 400 clinical studies including, breast cancer, prostate cancer, lung cancer, colorectal cancer and hepatocellular carcinomas.<sup>28-32</sup> The incidences and the types of cancers across the globe demarcates the regional socio-economical strata. For instance, Head and Neck cancer (HNC) prevalence in India is the highest in the world due to various factors, including tobacco use. A recent study by Khandare et al. showed that among the Indian population, CTC presence correlates with numerous clinicopathological parameters in HNC, particularly oral squamous cell carcinomas, and therefore, the use of CTC numbers as a viable indicator for establishing clinical staging in HNC patients (**Figure 2c**).<sup>33, 34</sup> This interest in the role of CTCs in metastatic progression and cancer disease management is emphasized by the 940 odd clinical trials (as of December 2020) conducted globally as referenced at [clinicaltrials.gov](http://clinicaltrials.gov). A significant number of these clinical trials addressing several critical aspects of CTC involvement in a multitude of carcinomas are aimed at evaluating the CTCs' clinical utility in three main areas: a) utilizing CTCs as surrogate tumor material for diagnostic evaluation from patient blood, b) assessing CTC numbers and changes in CTC counts during therapeutic

intervention, and c) targeting unique CTC specific biological features relating to metastatic progression. Phase III clinical trials such as SWOG S0500, CirCe01 (NCT01349842), DETECT-III (NCT01619111), and STIC-CTC (NCT01710605) in breast cancer and VISNU-1 (NCT01640405) in colon cancer have/are correlating CTC relevance in guiding chemotherapeutic decisions.<sup>35</sup>

Consequently, CTCs represent a central biomarker isolated from peripheral blood through non-invasive blood sampling, referred to as 'liquid biopsy.' Thus, CTCs offer a higher prognostic value for cancer progression prediction and therapeutic response monitoring.<sup>32, 36</sup> Detection, identification, and molecular characterization of CTCs thus play a pivotal role in unprecedented insights into the metastatic process. The potential clinical benefits associated with CTC detection and characterization and the ever-evolving understanding of material chemistry and tumor biology have been utilized to design various platforms for the static and dynamic enrichment of CTCs.

#### The role of circulating tumor cells in cancer metastasis.

Primary solid tumors are known to shed about 1 million CTCs per gram of tumor mass daily.<sup>29-31</sup> However, amongst billions of blood cells, the occurrence of CTCs is extremely low (1 CTC per  $10^7$  leukocytes per ml of blood), thus making them extremely rare.<sup>32, 36</sup> While disseminating from the primary tumor site and entering into blood circulation, CTCs undergo both genotypic and phenotypic changes through a phenomenon known as epithelial-mesenchymal transition (EMT).<sup>39</sup> Once in the circulatory system, CTCs exhibit varying phenotypic characteristics, namely, stemness (i.e., tumor-initiating properties), epithelial (i.e., adhesion), and mesenchymal (i.e.,

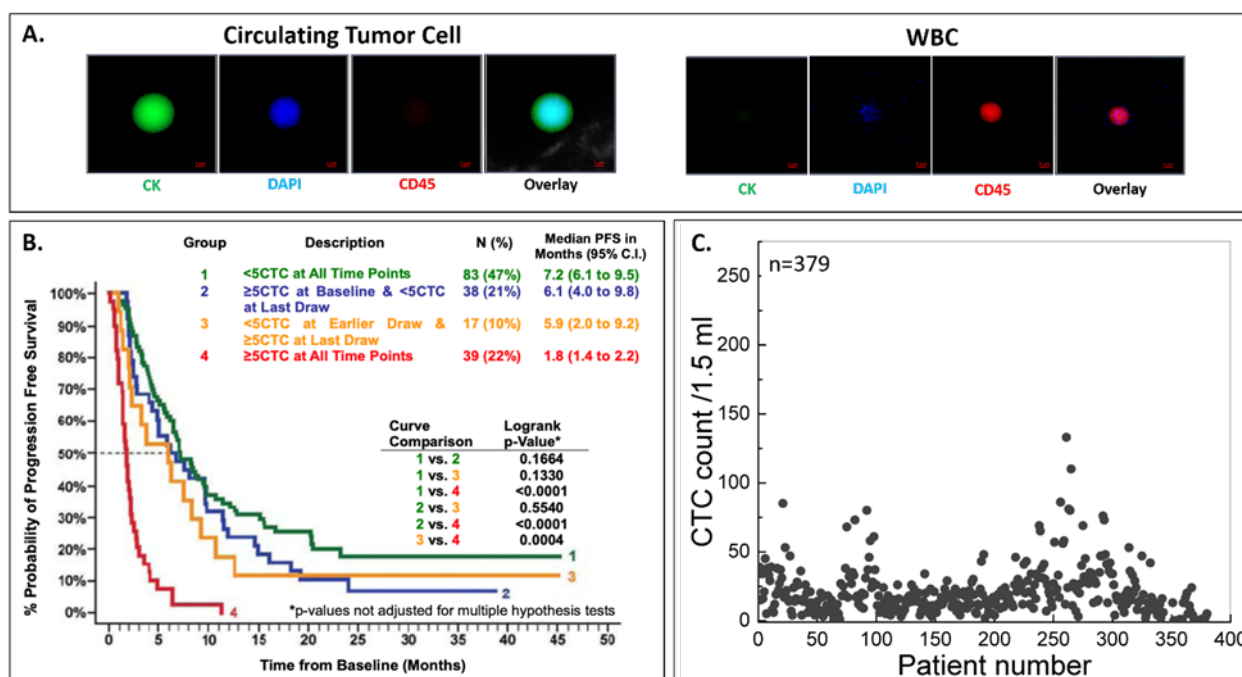


**Figure 2:** Clinical significance and outcome by CTC numbers, time from baseline in carcinomas. A) Representative CTC and white blood cell (WBC) images isolated from cancer patient blood sample. Immunostaining performed with FITC labelled anti-cytokeratin antibody, and AlexaFluor 555 labelled anti-CD45 antibody. 4',6-diamidino-2-phenylindole (DAPI) was used for nuclear counterstaining of CTC and WBC. CTCs indicate positive CK staining and negative CD45 staining. WBCs are positive for CD45 and negative for CK. Both cells are positive for nuclear stain. Scale bars represent 5  $\mu\text{m}$ ; B) Reduction in CTC number below 5 after therapy initiation predicts more prolonged progression-free survival (PFS), whereas an increase in CTC count to 5 or higher predicts shorter PFS in metastatic breast cancer (mBC) patients. The PFS graph indicates that patients with  $\geq 5$  CTCs at all time points (Group 4) showed the least median PFS, which was significantly decreased compared to Groups 3, 2, and 1, respectively.<sup>37</sup> C) Clinical correlation of CTCs as a blood biomarker of disease progression in Indian HNC patients. CTC distribution of 379 Head and Neck Squamous Cell Carcinoma (HNSCC) patients. The mean CTC number distribution is 21. Correlation of CTC presence and clinicopathological disease parameters implicates the use of CTCs in establishing clinical staging in HNC patients.<sup>33, 38</sup>

migration and invasion) properties. After that, CTCs tend to aggregate (up to  $> 100$  cancer cells) along with different cell types, that may include different immune cells, platelets, and cancer-associated fibroblasts. These extremely rare CTC clusters have aggressive metastatic potential that is assessed to be 23-50 times higher than single CTCs.<sup>32, 40</sup> CTC clusters, compared to single CTCs, have shorter circulation half-life. Also, the larger size of the cluster as compared to a single CTC is reported to enhance their rapid entrapment within blood capillaries of distant organs, where they could extravasate and activate metastasis under tumor favorable tissue microenvironments.<sup>32, 40</sup>

From the standpoint of survival and diagnosis, CTCs undergo unfavorable exposure in the bloodstream due to shear force (physical stress), anoikis, immune surveillance, apoptosis, and lack of growth factors. As a result,  $<0.01\%$  of CTCs are known to survive and extravasate at favorable distant sites to seed secondary tumor growth.<sup>41</sup> The extravasated cells must undergo a reversal to their prior epithelial phenotype by reverse EMT - the mesenchymal-epithelial transition (MET) to activate metastasis at the distant organs.<sup>28</sup> Together, EMT and MET phases represent transitory stages of cancer cells that result in heterogeneity of CTCs during the metastatic cascade. All such

transitions correlate in real-time with favourable and unfavourable disease prognosis directly implying the PFS, DFS and OS of the cancer patient (Figure 2b).

#### Approaches and challenges in CTC isolation technologies.

In 1869, Ashworth first described CTC presence in metastatic cancer patient blood. To date, a variety of strategies involving either biophysical or biochemical approaches have been developed for CTC isolation.<sup>42</sup> Biophysical-based methods depend on the transformations in the physical properties of CTCs paralleled to normal blood cells, including cell size, density, and deformability. Size-based filtration and density gradient centrifugation are two typical established biophysical methods used for CTC isolation and enrichment. Conversely, biochemical-based approaches involve selective CTC isolation by immunoaffinity capture of unique cancer-specific biomarkers such as Epithelial Cell Adhesion Molecule (EPCAM), Human Epidermal Growth Factor Receptor 2 (HER2), Folic Acid Receptor (FR), Transferrin Receptor (TfR) that are overexpressed on the CTCs' surface. Positive identification of CTCs may be achieved by fluorescence microscopy using differential fluorescent antibodies to detect the presence of Cytokeratins (CK) (e.g., CK8, 18, 19, etc.), which are

overexpressed in nucleated tumor cells (i.e. positive for nuclear counterstain DAPI) and for the absence of CD45 - a leukocyte surface biomarker. An event is positively confirmed as a circulating tumor cell when it exhibits tumor cell morphology and an EpCAM<sup>+</sup>, CK<sup>+</sup>, DAPI<sup>+</sup>, and CD45<sup>-</sup> phenotype (**Figure 2a, Figure 3**).<sup>43</sup>

However, low numbers in blood and high heterogeneity are significant challenges associated with efficient isolation and characterization of CTCs. There occurs variability in size, shape, deformability, surface expression of cell surface tumor-specific biomarkers, etc. across and within CTC populations of diverse cancer subtypes, in different cancer patient, and at various disease stage time points.<sup>44</sup> For cancer metastasis, studies at the cellular, proteomic, and genetic levels demand the isolation of CTCs in high numbers using platforms capable of higher specificity and efficiency. These limitations can be overcome by employing CTC enrichment methods with higher specificity and by minimizing contaminating normal hematopoietic cell fractions, thereby increasing the number of enriched CTCs.

Broadly, these methods can be classified as i) Positive enrichment, which captures the target CTCs and elutes other blood components such as clinically validated anti-epithelial cell adhesion antibody (anti-EpCAM) platforms, and ii) Negative enrichment, which captures the non-target normal blood cells (viz. erythrocytes (RBCs), leukocytes (WBCs), platelets, etc.) and elutes the target cells (i.e., CTCs). Positive enrichment technologies have many advantages, such as shorter CTC enrichment processes and retrieval of intact CTCs with minimal to no damage to cellular properties. Concomitantly, one of the significant limitations of approaches using negative enrichment of CTCs is the requirement of a considerable variety of antibodies required to eliminate normal hematopoietic constituents, thereby making the process expensive and also yielding low purity and specificity in the eluted CTC fraction, thus putting it beyond the scope of this review.<sup>45</sup>

Considering the critical challenges encountered in developing CTC isolation technologies, positive enrichment approaches utilizing nano/micro substrates conjugated to tumor-specific biomarkers have emerged as a predominant CTC isolation technique. Therefore, this review emphasizes the positive chemo-based CTC enrichment approaches and highlights the advances in chemistry design interface of various CTC capturing materials and its effect on the specificity and efficiency of CTC isolation and enumeration. The review highlights the existing multi-component materials involving different nano/micro-based substrates conjugated to cell surface biomarkers in different spatial arrangements. In subsequent sections, we review the chemistry of dynamic systems and technologies for CTC isolation and detection. We also briefly describe the material design for the post-capture release of CTCs, which could be further useful for downstream analysis at the cellular, proteomic, and genomic levels.

#### **Genomic profiling of CTC as liquid biopsy tools for next-generation cancer detection.**

Over the last couple of decades, a vast volume of research has highlighted the clinical utility of CTCs prognostic markers as a

vital factor in monitoring cancer progression. However, CTC's real potential for personalized cancer disease management can be realized through its molecular and genomic characterization. This is because genomic profiling of CTCs can non-invasively recapitulate the primary and metastatic tumor constitution, which otherwise is not available from the tissue biopsy due to highly variable clinical behavior of the same type of cancer in different patients. CTC analysis at a molecular and genomic level can provide a plethora of information (**Figure 4**) such as cancer marker heterogeneity among the CTC population, temporal variations in key metastatic regulators, presence and changes in stem cell marker expression, and dynamic variation in the therapeutic target expression.<sup>46, 47</sup>

Additionally, molecular profiling of CTCs is extremely valuable to better understand the epithelial to mesenchymal transition, a hallmark process of metastatic spread of the disease. Recent efforts for CTC characterization at the molecular and genomic level highlight their role in personalized cancer care. Gambhir et al. have demonstrated the development and clinical utility of a novel nano platform that integrated magnetic isolation of CTCs and a nano well array to isolate and sort thousands of CTCs at the single-cell level. Through this platform, EGFR, telomerase reverse transcriptase (TERT), and MET mutations and expression profiles could be detected heterogeneously among CTC populations originating from non-small cell lung cancer (NSCLC).<sup>48</sup>

Recently, Wang et al. observed a clear mutational heterogeneity in CTCs isolated from different epithelial tumors indicating the mutation is extremely different from the primary tumor.<sup>49</sup> This observation enabled the authors to understand the genetic and mutational heterogeneity based on single and multiple gene mutations in CTCs and the primary tumor. Efforts are ongoing to understand bloodborne metastasis by profiling CTCs obtained from breast cancer patients. In a seminal study, Park et al. performed expression profile and genome-wide copy number analysis on breast cancer CTCs.<sup>50</sup> Surprisingly, the EpCAM expressing CTC population did not display a breast cancer stem cell attributed phenotype. Further, most of the CTCs expressed estrogen receptor 1 (ESR1) compared to HER2, and their expression pattern showed considerable changes compared to cells of the primary tumor.

A recent clinical study involving the gene expression profile of CTCs was observed to be strongly correlated with the clinical outcome of head and neck cancer. Patients with CTCs strongly expressing or downregulating PI3K, MET, EGFR, ALDH1, CD44, CD47, and CD274 genes significantly correlated with treatment resistance, locoregional recurrence, and PFS. Further, a subpopulation of cancer patients with CD274 expressing CTCs had better PFS compared to patients with CD274 negative CTCs.<sup>51</sup>

Genetic analysis of CTCs is equally useful to understand the therapeutic potential of certain treatment regimens. In a prospective study, molecular profiling of CTCs from melanoma patients receiving combinatorial immunotherapy suggested that patients with CTCs expressing mutated BRAF and  $\beta$ -catenin were at high risk of poor therapeutic outcome.<sup>52</sup> Recently, Pantel and co-workers performed in-depth characterization of

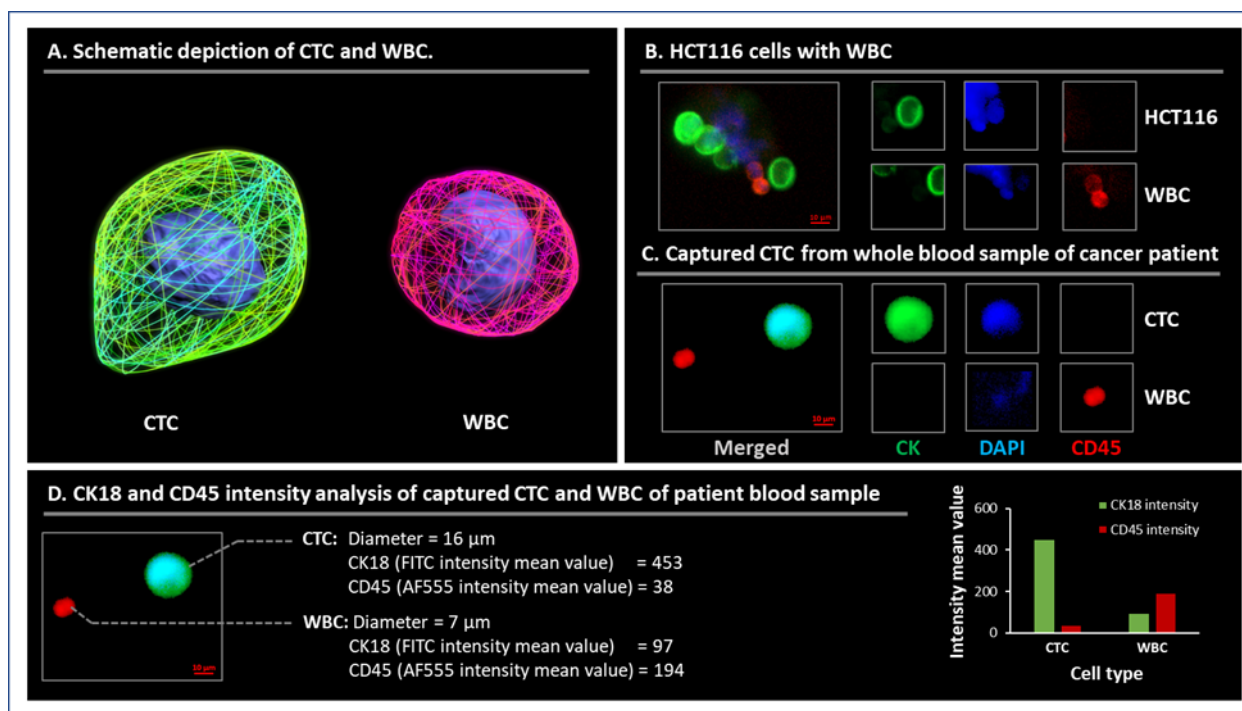


**Figure 3:** The differential characteristics of CTCs and WBCs. A) CTC and WBC illustrating CTC-specific, cytoplasmic, overexpressed CK proteins (green), WBC surface-expressed leukocyte specific antigen-CD45 (red), and nucleus (blue). B) Blood sample containing spiked HCT116 colorectal carcinoma cells, depicting characteristic CK and nuclear staining patterns using FITC-labelled anti-CK antibody and DAPI. WBCs stain positive for CD45 and nucleus (AlexaFluor555 labelled anti-CD45 antibody) but are negative for CK. C) Cancer patient blood sample with  $CK^+DAPI^+CD45^-$  CTCs and  $CD45^+DAPI^+CK^-$  WBCs. D) Size and immunofluorescence intensity differentiation of CTCs depicting the larger cell diameter and higher CK18 expression and lower CD45 fluorescence intensity mean values (IMV) than WBCs. The graph represents IMV differences of CK18 and CD45 between CTCs and WBCs. Scale bar represents 10 μm.

CTCs obtained from breast cancer patients that showed high metastatic and tumorigenic properties. Genetic analysis on these CTCs indicated that the cells retained high estrogen receptor (ER) expression ability and maintained a similar copy number variation profile compared to primary tumors. Further, down-regulation of ER signalling was constitutively active, impartial of ligand accessibility in CTCs and cyclin-dependent kinase inhibitors strongly inhibited CTC growth when cultivated *in vitro*.<sup>53</sup>

In addition, the characterization of protein markers on CTCs is valuable in clinical settings and can be readily achieved by flow cytometry or fluorescence microscopy. For example, dual Ki67/PSA (prostate-specific antigen) staining in CTCs of prostate cancer patients demonstrated increasing proliferation index in patients progressing from a responsive to a more refractory resistant disease form.<sup>54</sup> Similarly, androgen-induced and suppressed prostate-specific membrane antigen (PSMA) dual staining clearly indicated androgen signalling status heterogeneity within CTCs before and after hormonal therapy.<sup>55</sup> However, care must be taken for multiplexed protein markers analysis in CTCs, as faulty antibody calibration due to signal intensity, background levels of markers expressed in a hematopoietic subpopulation of other cells, and cross-reactivity of antibodies can easily skew the results. This could be one of

the prudent reasons why genomic characterization for molecular profiling of CTCs is fetching more popularity. Moreover, emerging novel liquid biopsies techniques and Next Generation Sequencing (NGS) has enabled mutational analysis and cancer disease profiling at the single CTC level, thereby providing unparalleled insights into the tumor heterogeneity, offering crucial aid to the clinical decision-making process. Use of label-free inertial microfluidics for efficient CTC capture without relying on EpCAM expression, combined with multiplexed targeted resequencing assays, such as the Illumina TruSeq® Amplicon - Cancer Panel that targets 48 cancer-related genes and 212 amplicons, has been highly efficient. It has enabled the genomic alteration analysis of CTCs from HNC and gastrointestinal cancer patients, as well as blood-based molecular profiling in identifying actionable drug targets, monitoring drug resistance, and tracking tumor dynamics and tumor DNA.<sup>56</sup> The earliest FDA approval for using such tests as a cohort diagnostic tool in clinical decisions for NSCLC therapy was granted in 2016 to the Roche cobas® EGFR Mutation Test v2. The test is based on real-time PCR that detects 42 mutations in specific exons of the EGFR gene from plasma or solid tumor samples. By 2020, qualitative NGS-based, pan-tumor liquid biopsy tests, such as the Roche-developed FoundationOne®Liquid CDx, have been granted FDA approval, thus further accelerating precision cancer therapy decisions in

certain types of prostate, lung, breast, and ovarian cancer patients. By providing comprehensive genomic profiling of about 300 cancer-associated genes and genomic signatures within tumor DNA, such multiplex diagnostic tests enable crucial treatment decisions for solid tumor management and treatment based on data obtained from liquid biopsies.<sup>37, 57</sup>

Nevertheless, cancer-specific antibody panels may eventually provide valuable information to monitor tumor progression status and guide clinical disease management and therapeutic decisions. Taken together, molecular and genomic profiling of CTCs establishes a unique biomarker and mechanism of cancer progression and treatment resistance. Indeed, CTC profiling can have high clinical utility as it provides seeming benefits over tissue biopsy, including non-invasive contact of serial monitoring. Further, genotyping of CTCs is likely to be useful for mutation-targeted therapies in lung (EGF and ALK mutations), skin (BRAF mutation), colorectal (EGFR and BRAF mutation), and breast (PI3K and HER2 mutations) cancers.<sup>58</sup>

Conversely, scientific progress has paved new avenues over the last decade, in terms of bio-marker based technologies for the detection of blood-based tumor-specific biomarkers, including CTCs, extracellular vesicles (e.g. exosomes) and circulating DNAs (e.g. cell-free DNA (cfDNA), circulating tumor DNA (ctDNA)). Numerous methodologies employing immunoaffinity, centrifugation (differential or density gradient), size exclusion chromatography, polymer-based precipitation, filtration, and molecular sieving have been developed into commercial exosome isolation technologies.<sup>59</sup> Similarly, for circulating DNAs numerous prior non-cfDNA isolation methods have been modified to specifically isolate cfDNA/ctDNA efficiently from cancer patient plasma samples.<sup>60</sup>

Tremendous efforts have been made to develop exceedingly sensitive liquid biopsy assays for detection and characterization of minimal residual disease (MRD), specifically to establish the presence of tumor cells that disseminate from a primary tumor site to distant organs. Such tests are particularly critical in patients who display no clinical or radiological signatures of overt metastasis or residual tumor cells lingering after local therapy, ultimately leading to local disease recurrence. Hence,

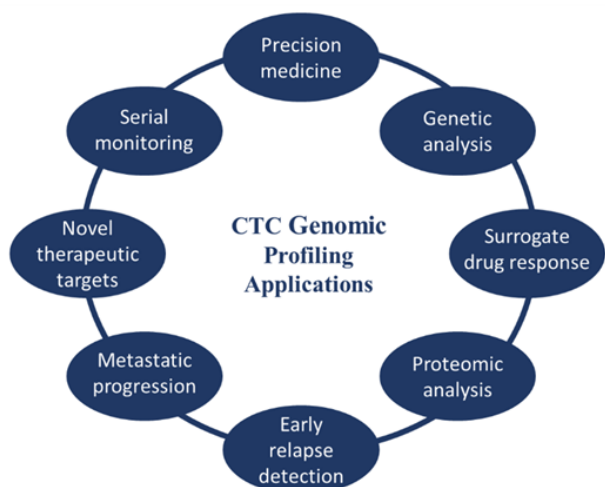


**Figure 4:** Clinical utilities of CTC genomic profiling in cancer disease management.

the detection of exosomes, cfDNA, ctDNA, or CTCs years following treatment is indicative of the persistence of MRD.<sup>61</sup> Liquid biopsy based approaches to detect a small number of CTCs at primary cancer diagnosis predicts an unfavorable prognosis. Therefore, risk stratification strategies are even more applicable in such circumstances aside from the current approaches to tumor staging. Further, CTC and ctDNA/cfDNA characterization offers valuable insights into MRD's molecular evolution during tumor progression, with therapeutic implications to delay or even prevent metastatic relapse.<sup>62</sup> DNA evaluation critically using plasma genotyping ascertains the primary mutations, chromosome aberrations, insertions/deletions, amplifications, rearrangements, and aneuploidy. Overall, these signatures assist oncologists for longitudinal disease monitoring, the ability to capture tumor heterogeneity, and interventional trials to further enhance clinical decisions and care.<sup>63</sup>

#### Chemo-functionalities for enhanced cell-specific targeting in isolation and enumeration of CTCs.

Nanomaterials bearing cell-targeting ligands, such as an anti-EpCAM antibody, transferrin (Tf), luteinizing hormone-releasing hormone (LHRH), sialic acid, folic acid are known to promote cell-specific topographic interactions with their counter-receptors, thereby assisting the capture, isolation, delivery, and recovery of cells.<sup>64</sup> Immobilization of targeting ligands (e.g., anti-EpCAM) on nanomaterials improves CTC recognition specificity significantly.<sup>65</sup> Furthermore, the nanomaterial's large surface to volume ratio endows high cellular binding affinity in the blood matrix. Fine tuning of nanomaterials contributes to multiplex targeting and detection, which are crucial to address the heterogeneous problem of CTCs.<sup>66</sup> Towards this, different types of nanostructured substrates, such as a magnetic nanoparticle, graphene, carbon nanotube (CNT), nanogel, cellulose nanocrystal, nanofiber, hyperbranched polymer, such as poly(amidoamine) dendrimer, and polyglycerol based platforms have been delineated (**Figure 1**).<sup>8, 67-70</sup> Moreover, some multi-component microfluidic substrates such as glass/polydimethylsiloxane (PDMS) assembly coupled to nanomaterial, further conjugated with CTC surface-specific markers have also been established as promising dynamic CTC isolation techniques (**Figure 5**).<sup>71, 72</sup> Such microfluidic assemblies can attain maximal ligand-target interaction by controlling the residence of time of cancer cell-containing fluid.

A diversity of organic functional groups such as amine, carboxylic acid, aldehyde, thiol, alcohol, etc., can be introduced on nano-substrates during or post-synthesis to render the ensemble reactive and specific. These functionalities offer basic colloidal properties to the nano-substrates, offer increased biocompatibility, enable conjugation with linkers such as small organic molecules, polymers, macromolecules, and finally introduce active biological moieties such as antibodies, DNA, and proteins. Some of the nano-substrates functionalized with small molecules followed by conjugation to the antibody using the most commonly used carbodiimide coupling are illustrated in **Figure 6**.<sup>73</sup>

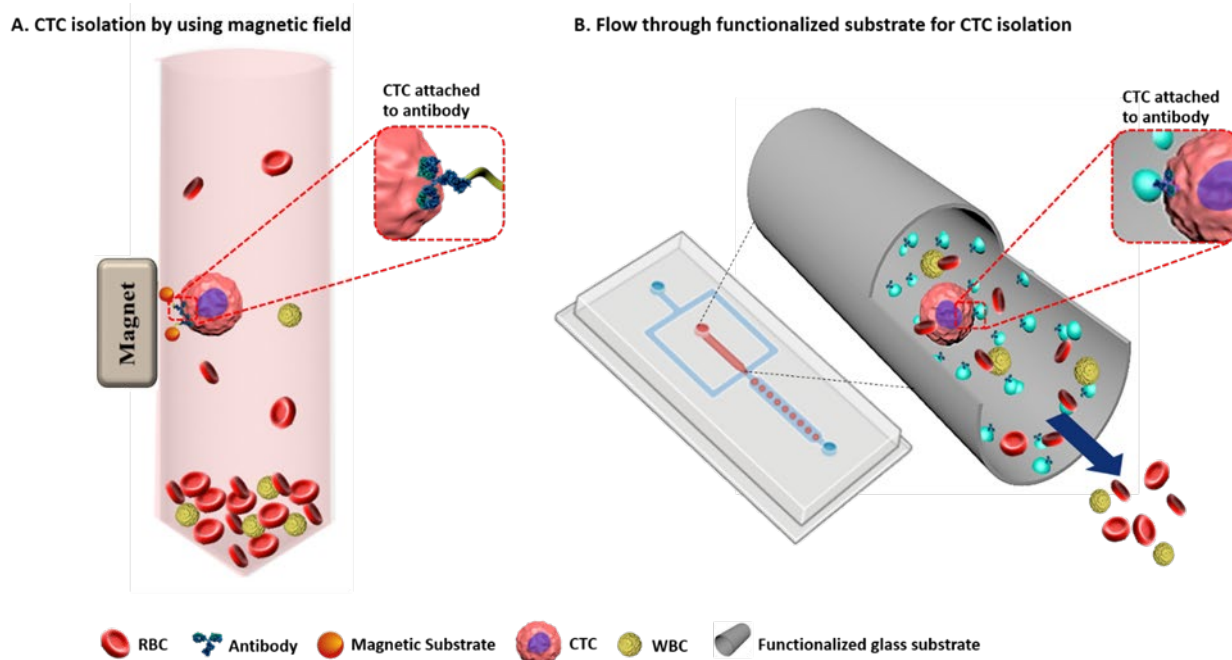


**Figure 5:** Schematics representing the two most commonly used methodologies for CTC capture, i.e., A) Static system: Immunomagnetic based CTC isolation; B) Dynamic flow-through system: Immuno-affinity-based CTC isolation.

Other than carbodiimide chemistry, various conjugation chemistry reactions have been employed for chemically introducing the targeting moieties (anti-EpCAM antibody) to the substrate directly or via a linker; for example, imine chemistry, isothiocyanate coupling, Diels-Alder reaction, hetero-functional reactions, iminothiolane reaction as depicted in **Figure 7**.<sup>74-77</sup>

The choice of selecting linkers is even more crucial when conjugating the substrates with targeting ligands (anti-EpCAM antibody, aptamer, DNA) as the linker enhances the proximity and probability of antibody-antigen interactions, thereby enabling high CTC capture efficiencies. For example, the long, flexible linker (PEG) or the multivalent, hyperbranched linker (polyamidoamine dendrimer (PAMAM)) allows enhanced local topographic interactions between the nanostructured material and cell surface components (e.g., EpCAM), ensuring a greatly improved cell-capture affinity in comparison with a short linker.<sup>78-82</sup>

Although capture and isolation of CTCs provide preliminary, diagnostically significant information, it is plausible that the molecular signatures and functional read-outs derived from CTCs can offer significant and valuable insights into tumor biology. This knowledge can produce highly beneficial outcomes if received at the critical moment where therapeutic intervention could make a substantial difference. To analyse CTCs at functional and molecular levels, it becomes crucial to develop materials that enable CTC capture with high efficiency and release CTCs with minimal contamination and insignificant disruption of CTC viability and cellular functions.<sup>75, 83-85</sup> In this context, using a stimuli-responsive linker or targeting ligand (DNA, aptamer) enables selective and gentle CTC release from capture substrates upon slight alteration of external conditions, thus enabling downstream CTC *in-vitro* analysis without the use

of harsh proteolytic digestion commonly employed to dissociate antibody-antigen interactions.<sup>83</sup> The commonly used stimuli-responsive linkers and their chemical structure have been described in **Figure 8** and discussed in detail in other sections of the review.

Apart from stimuli-responsive linkers, targeting ligands, such as aptamers, are also utilized in CTC isolation methodologies, as CTC release post-capture is easily achievable. Aptamers are considered “chemical antibodies,” which are short, single-stranded DNA or RNA molecules possessing unique tertiary structures that enable them to bind target moieties (ions, proteins, small molecules, macromolecules, tissues, cells, etc.) with enhanced affinity and specificity comparable to that of an antibody/antigen interaction.<sup>86,87</sup> In the CTC isolation and analysis field, aptamers have demonstrated increasing potential as alternative recognition ligands to antibodies, which may be scarce due to limited knowledge and availability of target antigenic cancer markers.<sup>87</sup> Consequently, many aptamers against cell-surface expressed cancer biomarkers have been developed, including EpCAM, HER2, EGFR, Mucin 1 (MUC1), Prostate-specific membrane antigen (PSMA), Carcinoembryonic antigen (CEA), etc.<sup>86, 88-91</sup> Furthermore, the ease of labelling and enhanced stability bestow added advantages for the aptamers utility in microfluidic chip-based systems for CTC isolation.<sup>86</sup> Additionally, the use of aptamers enables the selective and gentle release of CTCs from capture substrates, thus allowing downstream CTC *in-vitro* analysis.<sup>83</sup> In this manner, the release of CTCs would preserve their inherent biological characteristics and greatly facilitate use in downstream applications, thereby enabling further CTC characterization on the cellular, proteomic, and genomic levels.

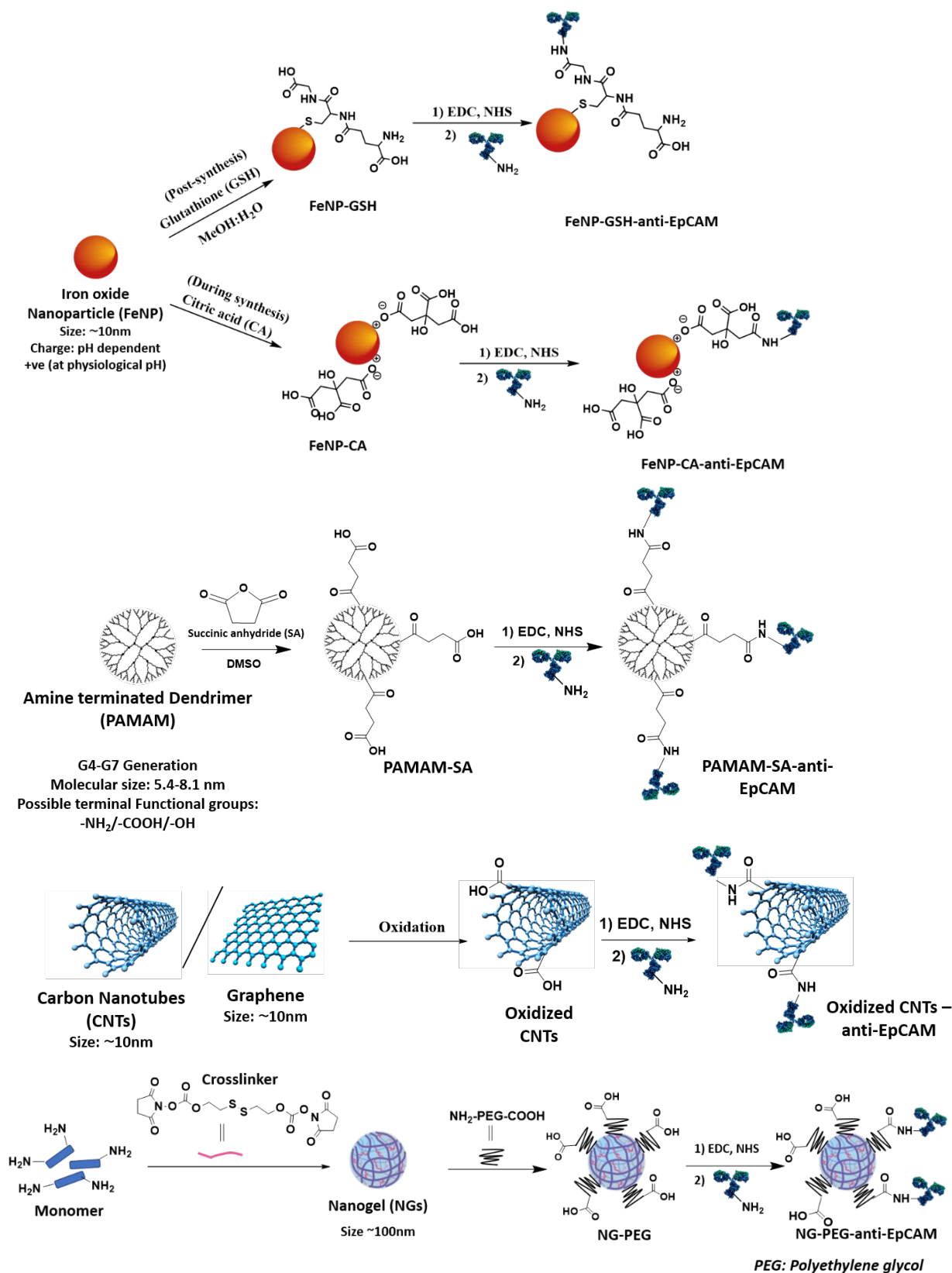


**Figure 6:** Schematic representation for the generation of reactive functionalities on the commonly used nano-substrates and linking targeting ligands for CTC capture and isolation. Acidic functional groups have been introduced onto the nano-substrates, followed by conjugating anti-EpCAM antibody by carbodiimide coupling using 1-Ethyl-3-(3-dimethylaminopropyl)carbodiimide (EDC), N-Hydroxysuccinimide (NHS).

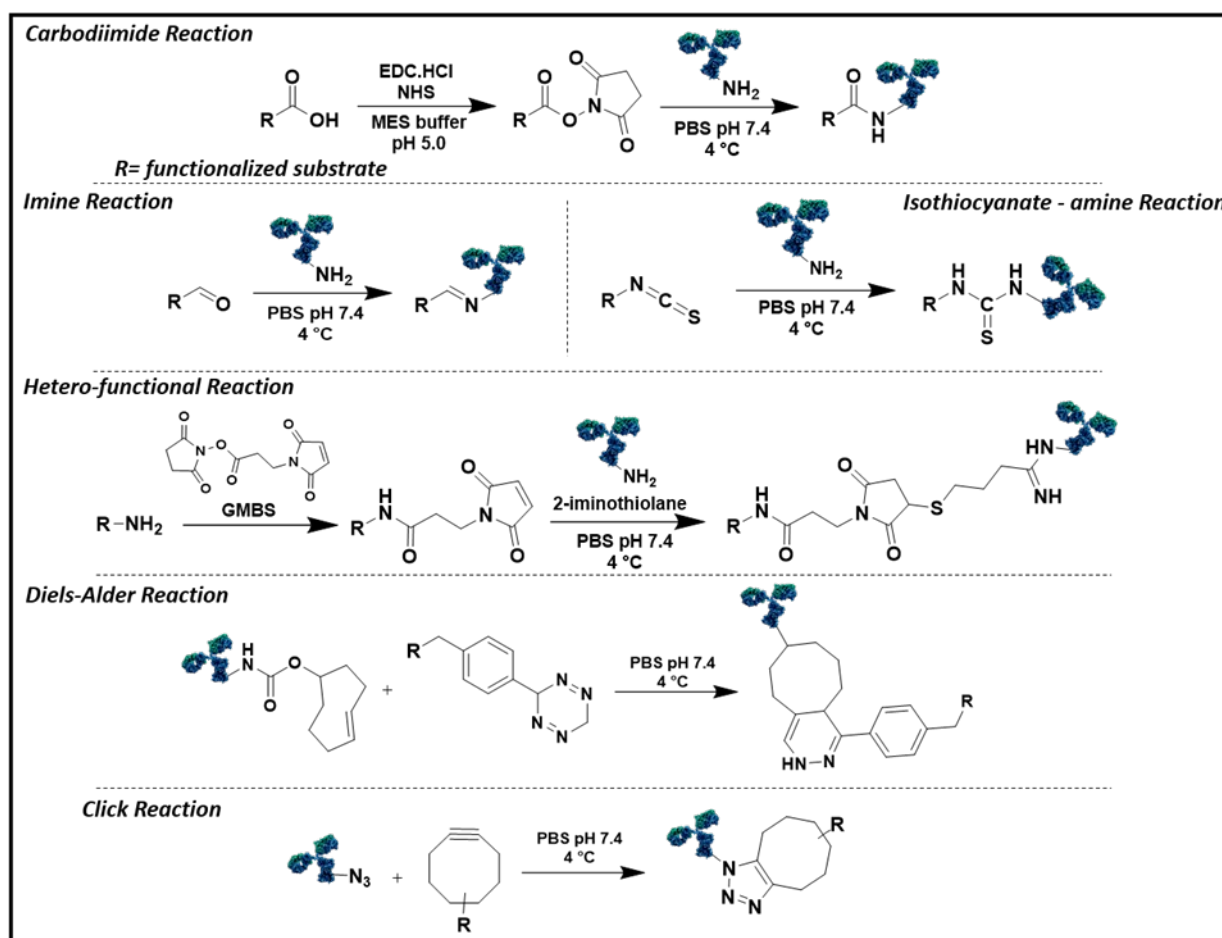


**Figure 7:** Commonly employed conjugation reactions for coupling nano/micro substrates, possessing different reactive groups with targeting ligands, e.g., transferrin and antibody.

### Tumor over-expressed surface biomarker proteins for targeting CTC isolation.

While advanced material interfaces are used to design CTC capture platforms, identifying overexpressed tumor-specific biomarkers is equally essential to ensure specific and efficient capture of CTCs. The tumor biomarkers commonly targeted when developing CTC isolation techniques have briefly been described below.

**Epithelial Cell Adhesion Molecule (EpCAM)** is a 39-42 kDa glycoprotein, which has been correlated with weaker cell adhesion, contact adhesion, and polarization, suggesting that EpCAM behaves as a negative regulator of adhesion; a hallmark of tumor cells.<sup>92, 93</sup> EpCAM was the first clinically validated biomarker shown to be overexpressed in numerous carcinomas and described as “a major epithelial carcinoma antigen.”<sup>94</sup> EpCAM tends to be highly overexpressed in multiple epithelial cancers like breast, ovarian, pancreatic, prostate, urothelial, gall bladder, head and neck cancers, etc. and at lower levels in normal epithelial cells.<sup>94-97</sup> High EpCAM expression is often correlated with disease relapse and decreased patient survival.<sup>95-97</sup> Owing to the prevalence of EpCAM overexpression in many carcinomas and CTCs, it has become a “gold-standard” target biomarker in cancer diagnostics, specifically CTC isolation/enrichment technologies.

The tumor biomarker’s significance in cancer diagnostics was realized in 2004 when the United States Food and Drug Administration (USFDA) approved the CellSearch® Circulating Tumor Cell Test for use in clinical diagnostic testing for CTC enumeration specifically in metastatic breast, colorectal, and prostate cancers.<sup>98, 99</sup> The immunoassay relies on immunomagnetic materials conjugated to a monoclonal antibody specific to EpCAM, enabling separation of the rare EpCAM overexpressing CTCs from the other blood cells that do not express the tumor biomarker.<sup>100</sup>

Additionally, in 2019, the Drug Controller General of India (DCGI) approved the OncoDiscover® Liquid Biopsy Test for clinical cancer diagnostics to detect, capture, and enumerate CTCs in low blood volume (1.5 ml) using immunomagnetic separation of EpCAM<sup>+</sup> tumor cells. Similarly, numerous methodologies to isolate CTCs rely on immunoaffinity-based targeting of this cell surface tumor antigen.

However, it is noteworthy that CTCs in some carcinomas are characterized by variable or negative EpCAM expression patterns (EpCAM<sup>-</sup> CTCs).<sup>92, 94, 101</sup> This has been attributed to genotypic and phenotypic changes occurring in CTCs owing to EMT, thereby leading to a downregulation of epithelial phenotype tumor markers (e.g., EpCAM, Cytokeratin, etc.) and upregulation of mesenchymal phenotype tumor markers (e.g.,

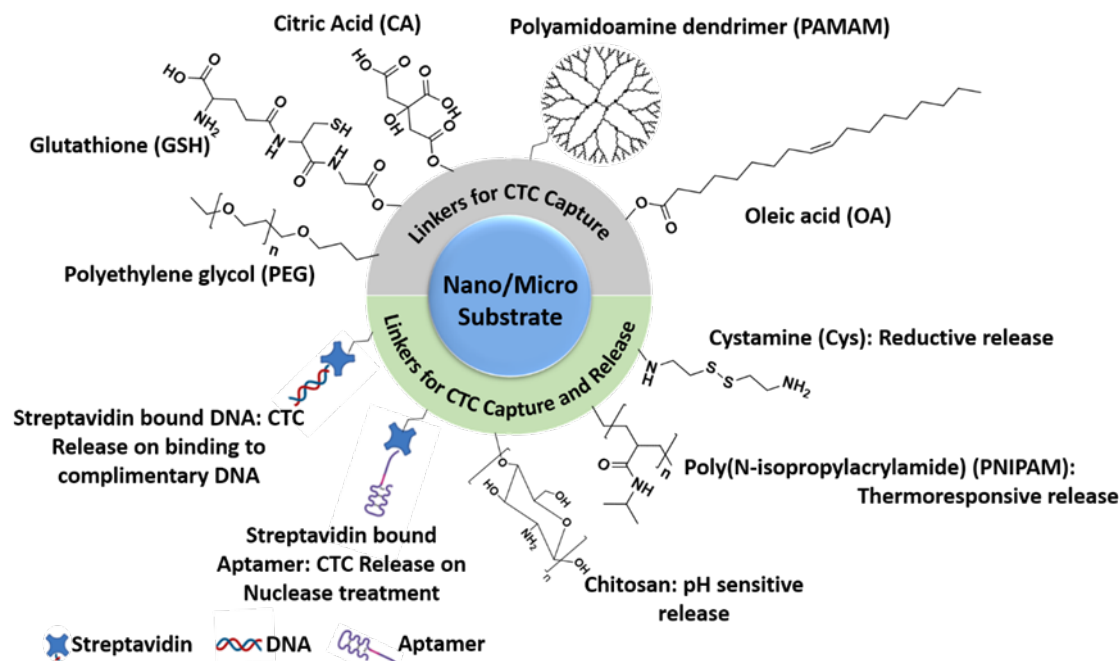


**Figure 8:** Chemical structures of commonly used reactive linkers for conjugating the nano/micro substrates with ligands to capture CTCs.

Vimentin, N-Cadherin, fibronectin, etc.).<sup>92, 102</sup> Therefore, methods relying solely on capturing CTCs that are EpCAM<sup>+</sup> will not efficiently account for CTCs that undergo EMT, thereby omitting certain subsets of CTCs. Consequently, other tumor markers have emerged as targets for CTC isolation.<sup>92</sup>

**Human Epidermal Growth Factor Receptor 2 (HER2; also called Neu/ErbB2)**, a 185kDa type I transmembrane growth factor receptor protein, is part of the EGFR group of tyrosine kinase receptors.<sup>103</sup> HER2 overexpression is predominantly reported in approximately 20–30% of human breast and ovarian cancers, generally associated with a more aggressive disease progression and worse patient outcomes.<sup>103–105</sup> Also, HER2 overexpression has also been documented in Wilm's tumor, bladder cancer, pancreatic cancer, colon tumor, and subtypes of esophageal, gastric, endometrial cancers associated with worsened disease status; and to a rarer extent in oropharyngeal, lung, and bladder cancers.<sup>104, 105</sup> When taken into consideration, HER2 overexpression across numerous carcinomas has become crucial in validating HER2 targeted CTC isolation strategies. However, like EpCAM-based CTC isolation strategies, the success of HER2-targeted CTC isolation relies solely on the type of carcinoma under-diagnosis and whether HER2 overexpression is a hallmark feature of that particular cancer.

**Folic Acid Receptor.** Folate deficiency is associated with numerous diseases, including cancers (e.g., breast, ovarian, colon, etc.). Folate receptors are cell surface, cysteine-rich glycoproteins that strongly bind folic acid (FA).<sup>106</sup> These receptors exist in three isoforms: FR $\alpha$ , FR $\beta$ , and FR $\gamma$ . Of the three isoforms, FR $\alpha$  is the most extensively studied. While FR $\alpha$  exhibits baseline expression in normal cells, it is highly overexpressed in numerous non-mucinous epithelial tumors.<sup>107</sup>

It is known that over 95% of ovarian cancer (OC) patients overexpress FR $\alpha$ , where increased FR concentration is associated with tumor progression and decreased survival.<sup>106</sup> Consequently, there is considerable interest in targeting FR $\alpha$  receptor overexpression on the CTC surface for their isolation; specifically, in OC and other non-mucinous epithelial tumors.

**Transferrin Receptor.** Transferrin (Tf) is an 80kDa glycoprotein and is part of a family of iron-binding blood plasma glycoproteins that binds ferrous iron (Fe<sup>3+</sup>) preventing it from travelling throughout the body in this form, which is toxic to cells, thereby transporting and delivering iron into cells by interactions with its Tfr.<sup>108</sup> Significantly upregulated expression of Tfr is observed on cancer cells in comparison to their normal counterparts.<sup>108</sup> This increase in Tfr expression is generally correlated with advanced tumor stage and poorer patient prognosis.<sup>108</sup> Consequently, these observations have validated Tf as a ligand model for the capture of Tfr<sup>+</sup> CTCs.<sup>109</sup> Therefore, numerous research groups have reported the use of Tf-conjugated substrates for CTC enrichment in both cancer cell lines and different cancer subtypes, including breast cancer, HNC, colon cancer, etc.<sup>109–113</sup>

Before clinical validations, the chemical-based CTC targeting substrates conjugated to tumor-specific targeting ligands are generally validated in cancer cell lines expressing tumor-specific biomarker proteins to test for specificity and efficiency of CTC enrichment. For example, the commonly used tumor cell lines overexpressing cell surface EpCAM protein are MCF-7, HCT 116, A549, Hep G2, etc. Additional examples of cancer cell lines and their overexpressing cancer biomarkers, along with their relevant targeting ligands, have been detailed in **Table 1**.

**Table 1:** Commonly used cancer cell lines utilized in CTC enrichment-based studies.

Cancer Cell lines	Cell Type	Overexpressed Cancer Biomarker	Capture Antibody/Ligand	Reference
MCF-7	Human breast ductal carcinoma	EpCAM	Anti-EpCAM	114-118
A549	Human lung carcinoma	EpCAM	Anti-EpCAM	117, 119-121
Panc-1	Human pancreatic ductal carcinoma	EpCAM	Anti-EpCAM	81
Hep G2	Human hepatocellular carcinoma	EpCAM	Anti-EpCAM	115
HCT116	Human colorectal carcinoma	EpCAM Tf-receptor	Anti-EpCAM/ Transferrin	111, 119
A431	Human epidermoid carcinoma	EpCAM EGFR	Anti-EpCAM/ Anti-EGFR	84, 119
SkBr-3	Human breast adenocarcinoma	HER2	Anti-HER2	115, 119, 122, 123
HeLa	Human cervical adenocarcinoma	Folate receptor	Folic acid	120

A schematic representation of different targeting ligands conjugated to a CTC capturing substrate via a chemical linker and their interaction with specific tumor overexpressed cell surface receptors present on CTC is represented in **Figure 9**. Generally, targeting ligands recognize molecular shapes and complementary sequences on cell surface receptors, and the better the fit in terms of geometry, the higher the affinity between them, ultimately leading to stronger interactions. These interactions between cell surface receptors and targeting ligand exclusively involve non-covalent bonds in a similar manner as enzymes bind to their substrates. These interactions are reversible and easily dissociated by high ionic strength or under extreme pH conditions.

## 2. Chemo-specific multi-component nanomaterials for CTC enrichment.

Designing multi-component nanomaterials can effectively enhance the sensitivity and efficiency of CTC capture enumeration and detection. Moreover, the inimitable properties of nanomaterials, as discussed earlier, can overcome the limitations of CTC detection. This section will focus on the material design interface with respect to magnetic nanomaterials, which are the gold standard in CTC isolation.<sup>125</sup>

## Functionalizing iron oxide magnetic nanoparticles for CTC capture.

The variety of applications engaging FeNP, such as labelling and magnetic separation of biological constituents, directed drug delivery, MRI contrast enhancement, hyperthermia treatment, has brought about a tremendous increase in designing their synthetic methodologies. The most relevant synthetic approaches include co-precipitation, thermal decomposition, sonolysis, sol-gel processes, spray and laser pyrolysis, hydrothermal and high-temperature synthesis, nanoreactors, and microwave-assisted synthesis.<sup>126-143</sup> Thus, to have the desired control over the physicochemical properties of nanoparticles such as size, shape, charge, stability, dispersibility, etc., it becomes highly essential to choose the synthetic methodology carefully.

Based on the size, magnetic particles are ordered as large (1.5 to about 50  $\mu\text{m}$ ), small (0.7-1.5  $\mu\text{m}$ ), or colloidal (<200nm); referred to as nanoparticles.<sup>144</sup> As known, magnetic enrichment is the favoured method for cell isolations, and the particles engaged in this process do not have to be removed prior cell analysis. Also, the particles should be small enough to not obstruct the analytical measurements, i.e. <200nm. Furthermore, the particle should be large enough and paramagnetic in nature to allow cell separation using external magnetic field. Additionally, the uncoated colloidal magnetic particles possess a suitably high positive charge at physiological pH (**Figure 10**). Therefore, a coating material should preferably be applied to prevent nonspecific interaction between the magnetic core and biological macromolecules, such as sialic acid residues on the non-target cell surface, lectins, glycoproteins, and other cell membrane components. Several base coating materials have been described in the literature, such as polymers, organic molecules, inorganic materials, and biomolecules. However, lately, the attention has shifted to molecules that can provide an additional and high-density iron nanoparticle functionalization to further the conjugation reaction (**Figure 10**).

Iron oxide nanoparticle-based enrichment methods are among the first and most widely used techniques to isolate, enumerate, and detect relevant tumor biomarkers such as CTCs *in vitro* from whole blood samples.<sup>145</sup> Immunomagnetic separation technique is advantageous due to exclusive magnetic properties including, easy handling with a magnet, possible surface coating, chemical coordination of reactive groups on FeNPs and further linking with bio-functional ligands of interest, higher surface-volume ratio, sufficient dispersibility in biological medium and relatively acceptable biocompatibility.<sup>98, 146, 147</sup> The immuno-magnetic affinity system involves FeNPs conjugated to targeting moieties, that evidence non-covalent interactions with CTCs and thus enable their separation via an external magnetic field.<sup>99</sup> In short, magnetic nanoparticles have been the most crucial platform in CTC enrichment techniques, and maximum CTC detection research is focused on using magnetic nanoparticles. Even the

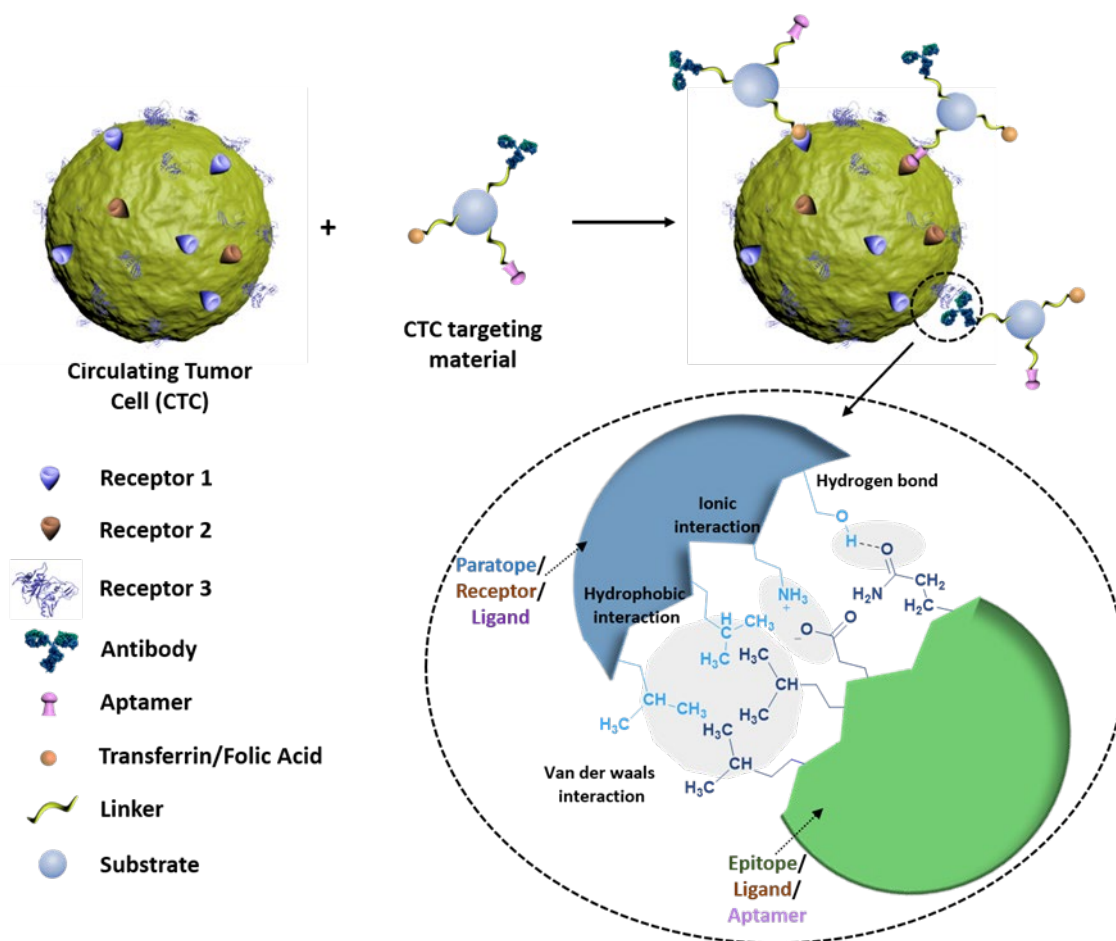


**Figure 9:** Schematics representing non-covalent interactions between CTC surface biomarker proteins and the biomarker targeting ligands conjugated to the nano/micro substrate. Information adapted from ref.<sup>124</sup>

commercialized technologies approved by regulatory bodies for CTC enrichment and detection utilize magnetic nanoparticles linked with anti-EpCAM antibodies, two of which are described below.

**CellSearch® Circulating Tumor Cells Test.** The CellSearch® system uses magnetic nanoparticles of size 90-150 nm coated with bovine serum albumin (BSA). The BSA-coated nanoparticles were then coupled to streptavidin with sulfosuccinimidyl 4-(N-maleimidomethyl)cyclohexane-1-carboxylate using heterobifunctional chemistry. For antibody coupling, monobiotinylated antibody was reacted with streptavidin magnetic nanoparticles for 1 hour. The remaining active streptavidin sites were blocked with biotinylated-BSA (Figure 11).<sup>98,99</sup> The use of multilayer protein (BSA, streptavidin) on nanoparticles reduces nonspecific interactions with other blood components compared to uncoated nanoparticles, and utilization of monoclonal antibody (anti-EpCAM) exhibits high specificity for a particular EpCAM epitope. The enrichment method comprises of mixing the blood sample of the cancer patient with colloidal magnetic beads coupled to antibody targeting the tumor-associated antigen (EpCAM) on the CTC surface,<sup>148</sup> but which does not enrich other cellular and non-cellular components of the blood above a baseline threshold of EpCAM expression. Subsequently, the blood-magnetic particle

mixture is subjected to a magnetic field to produce a cell fraction enriched in antibody-coupled magnetic particles bound CTCs. Finally, the enriched fraction of CTCs is analyzed. The tumor cells present in the sample can be characterized by cellular and molecular markers to determine prognostic and predictive disease status. This system utilizes automated digital microscopy to identify and enumerate CTCs and is proved to have a sensitivity of 87.7%. The CellSearch® system has been widely accepted in clinical utility, however, with few limitations, i) the detection cost is very high as CellSearch® uses biotinylated monoclonal antibodies, ii) the CTC isolation is challenging for heterogeneity molecular analysis and phenotype identification since this system primarily captures EpCAM<sup>+</sup> cells, iii) the sensitivity and selectivity are comparatively low.<sup>149</sup>

**OncoDiscover® Liquid Biopsy Test.** Recently, an immunomagnetic affinity-based CTC diagnostic test was approved by the Central Drugs Standard Control Organization (CDSCO, India) for detecting epithelial cancer cells from bladder, prostate, neuroendocrine, liver, pancreatic, lung, breast, head and neck, colorectal, ovarian, and stomach.<sup>33, 34, 38, 147</sup> The OncoDiscover® Test, based on the OncoViu® platform, uses a multi-component system consisting of glutathione-linked iron nanoparticles covalently conjugated to carbon allotropes like CNT and graphene via PAMAM dendrimer as a linker. Finally,

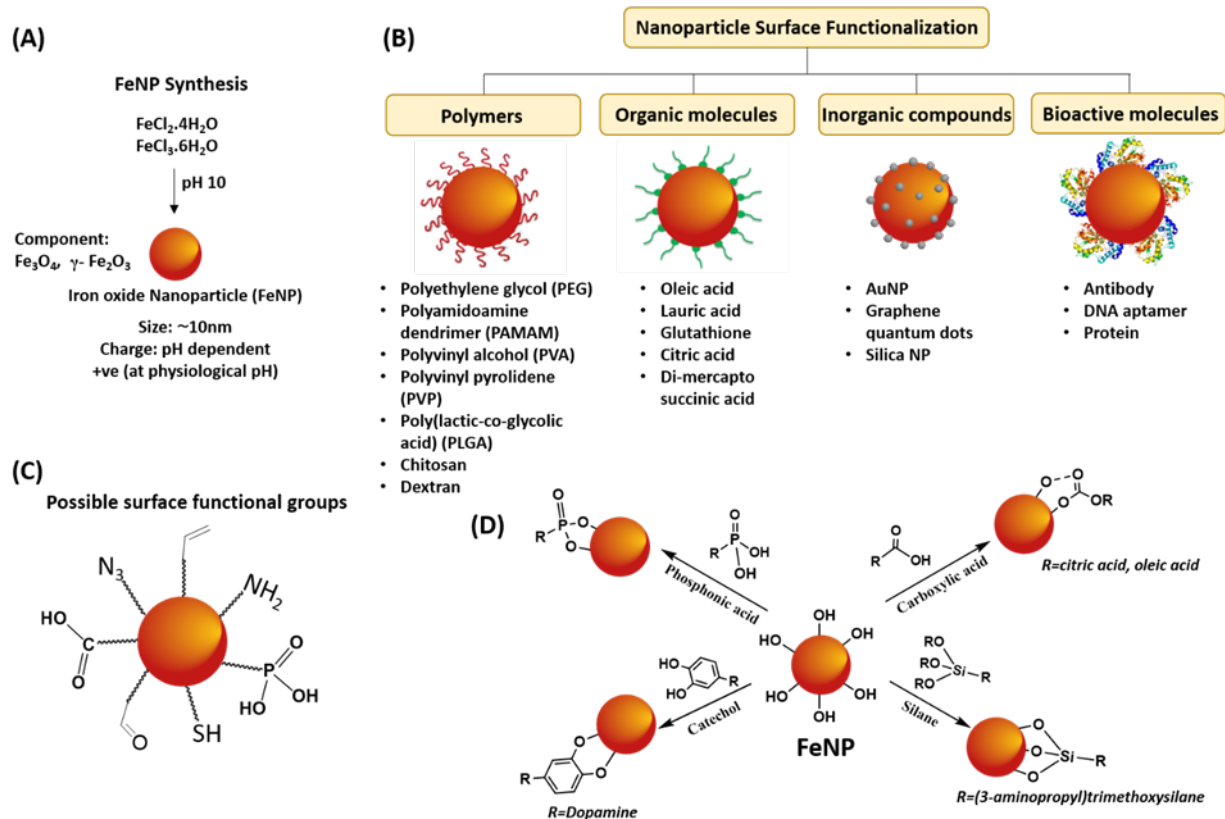


**Figure 10:** Schematics for surface functionalization of FeNP. A) Preparation by co-precipitation method; B) Coating and surface functionalization; C) Possible reactive groups; D) Schematic illustration showing the introduction of organic functionalities on FeNP.

the iron NP-CNT substrate is decorated with optimized amount of EpCAM antibodies via carbodiimide chemistry (Figure 12). The multi-component system provides a high density functional

groups for anti-EpCAM antibody immobilization, thus, increasing the availability of cell recognition sites resulting in enhanced cell capture efficiency. The OncoDiscover<sup>®</sup> test

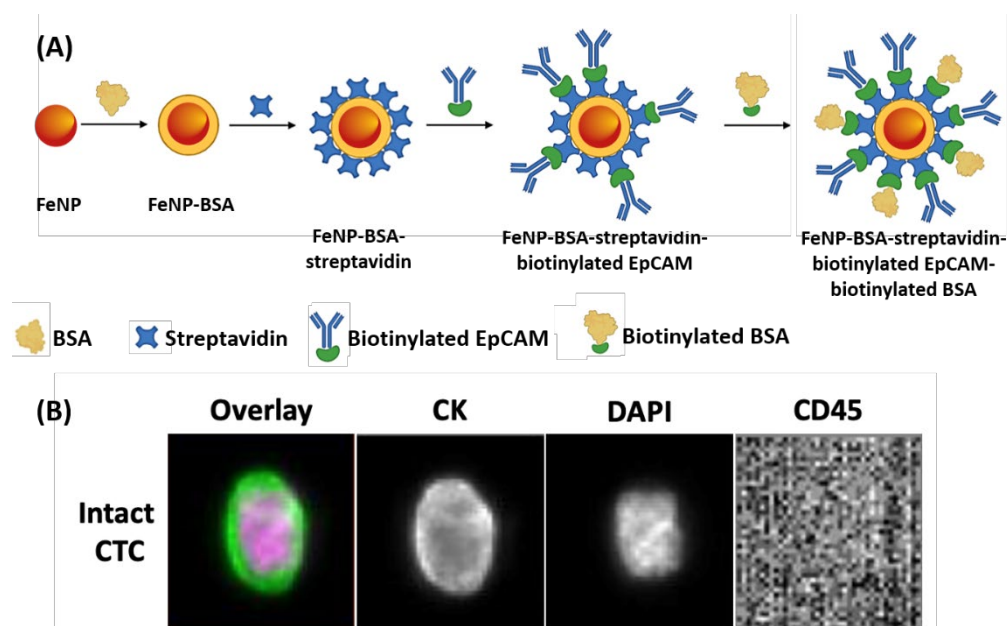


**Figure 11:** A) Schematics of surface functionalization of FeNPs with targeting ligand utilized in the CellSearch<sup>®</sup> Circulating Tumor Cell Test; B) Representative image of intact CTC isolated from NSCLC patient blood using CellSearch<sup>®</sup> Circulating Tumor Cell Test. CTC is positive for CK staining as well as nuclear stain DAPI but negative for leukocyte antigen CD45. Adapted from ref.<sup>150</sup>

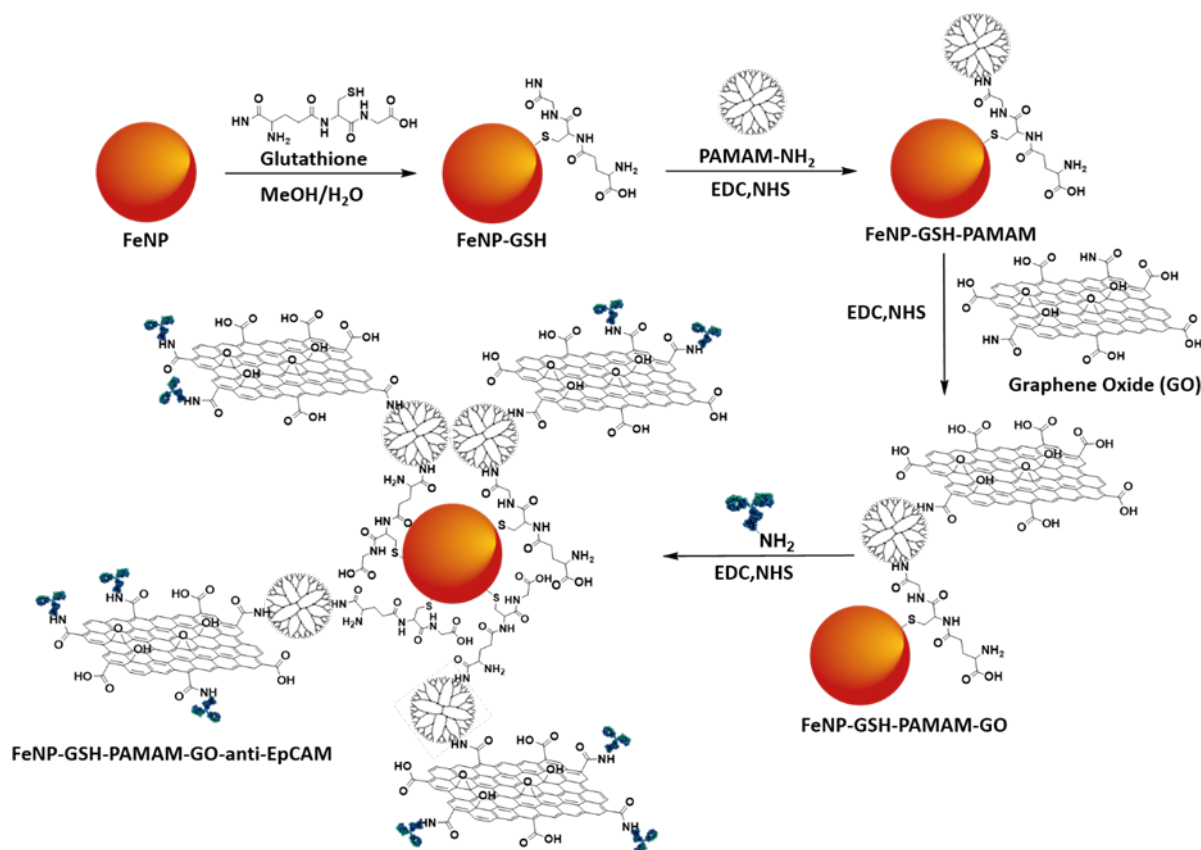


**Figure 12:** Preparation of multi-component material for isolation of CTCs using OncoDiscover® Test. Multivalent linker (PAMAM), graphene oxide (GO) sheets, anti-EpCAM have been conjugated onto glutathione coated FeNP using carbodiimide coupling reactions.

immunomagnetically enriches cells overexpressing EpCAM. The captured cells expressing Cytokeratin 18 are characterized by the immunofluorescence (IF) method using a combination of fluorescent dyes (anti-cytokeratin and anti-CD45). The *in-vitro* diagnostics test rapidly isolate, detect, and enumerate CTCs with high precision, specificity, and efficiency.<sup>151</sup>

Such commercial technologies have been engineered on the advances made in recent years in the field of material designs. A summary table of the commercially approved CTC isolation and detection technologies has been represented in **Table 2**.

Racila et al. reported the first use of magnetic NPs for enrichment, detection, and characterization of carcinoma cells in the blood.<sup>145</sup> Since then, much advancement has been substantiated in the material interface to decrease the nonspecific interaction to increase the bio-specificity towards the targeting marker. For example, Ding et al. established a method for efficient capture and sensitive fluorescent labelling of CTCs based on near-infrared fluorescence Ag<sub>2</sub>S (silver sulphide) nanodot-based signal amplification combined with immunomagnetic spheres.<sup>114</sup> The design consisted of the anti-EpCAM antibody conjugated on the surface of oleic acid stabilized magnetic nanoparticles via carbodiimide coupling. Oleic acid prevents the iron nanoparticles from agglomeration and protects them from unwanted interaction with blood samples. In addition, these magnetic nanospheres labelled anti-EpCAM antibodies showed high capture efficiency (>95%) of

CTCs, with a lower limit of 6 CTCs, in MCF-7 cells spiked blood samples.

In an exciting publication, Haun et al. delineated a bio-orthogonal nanoparticle detection (BOND) method, demonstrating the employment of the Diels-Alder reaction for CTC enrichment.<sup>119</sup> The process employed a simple, rapid, and catalyst-free cycloaddition Diels-Alder reaction interfacing tetrazine (Tz) and transcyclooctene (TCO). The authors used a BOND chemistry-based system for labelling carcinoma cells using a two-step approach: antibodies targeting biomarkers of interest (EpCAM, HER2, EGFR) were conjugated with transcyclooctene and incubated with cell lines (HER2 for SK-BR-3, EpCAM for HCT 116 colon cancer cells, and EGFR for A549 lung cancer cells). Then, transcyclooctene modified cells were then directly resuspended with tetrazine modified magnetic nanoparticles (MNPs) to couple via cycloaddition reaction (**Figure 13**). Since multiple tags could modify one antibody without compromising its affinity, multiple attachments of Tz-MNPs to cells were achieved utilizing the antibodies as scaffolds. Therefore, parallel to the cell-MNPs preparation method directly using MNP-antibody conjugates, the two-step BOND strategy was efficiently amplified by MNP-binding to cells leading to enhanced efficiency and detection sensitivity. The material was validated with different antibodies (Anti-HER2, anti-EpCAM, anti-EGFR antibody) against various cell lines (HCT 116, SK-BR-3, A549, NCI-H1650, A431, etc.).

**Table 2:** Commercially available, clinically validated CTC diagnostic technologies.

CTC Enumeration Technology	Company	Country Approved	Regulatory Approving Agency	Principle	Pros	Cons
CellSearch® Circulating Tumor Cell Test	Menarini Silicon Biosystems, Italy.	USA China	USFDA	Immunomagnetic positive enrichment	<ul style="list-style-type: none"> <li>Convenient.</li> <li>Highly specific.</li> <li>High enrichment efficiency.</li> <li>Routine blood withdrawal required.</li> </ul>	<ul style="list-style-type: none"> <li>Low CTC detection rate</li> <li>Detects only EpCAM<sup>+</sup> expressing CTCs.</li> <li>Risk of false positives and false negatives.</li> <li>Requires a large blood volume (7.5 ml).</li> </ul>
OncoDiscover® Liquid Biopsy Test	Actorius Innovations and Research Pvt. Ltd., India.	India	CDSCO (DCGI), India	Immunomagnetic positive enrichment	<ul style="list-style-type: none"> <li>Convenient.</li> <li>Highly specific.</li> <li>Small blood volume (1.5ml) required.</li> </ul>	<ul style="list-style-type: none"> <li>Detects only EpCAM<sup>+</sup> expressing CTCs.</li> <li>Risk of false positives and false negatives.</li> </ul>
ADNA Test®	AdnaGen AG, Germany.	Germany	N/A	Immunomagnetic positive enrichment	<ul style="list-style-type: none"> <li>Superior CTC detection rate due to PCR verification of tumor specific transcripts.</li> <li>High specificity.</li> </ul>	<ul style="list-style-type: none"> <li>Large volume of blood (10 ml) required.</li> <li>Scalability as time from blood draw to analysis is critical.</li> </ul>
ISET® Blood Cytopathology Test	Rare Cells Diagnostics, France.	France	N/A	Antibody-independent whole blood filtration	<ul style="list-style-type: none"> <li>Size based approach can enable detection of heterogenous CTC population</li> <li>High sensitivity.</li> <li>Can distinguish between single CTCs and CTC clusters.</li> </ul>	<ul style="list-style-type: none"> <li>Smaller sized CTCs may be lost.</li> <li>Leukocyte contamination.</li> <li>Lower specificity.</li> </ul>
CellCollector®	GILUPI Nanomedicine GmbH, Germany.	Germany	CE-marked	Antibody-based (EpCAM) positive enrichment using gold coated medical grade stainless-steel wire	<ul style="list-style-type: none"> <li><i>In vivo</i> CTC isolation from patient blood stream.</li> <li>No blood volume limitations.</li> <li>Increased sensitivity.</li> <li>High efficiency.</li> <li>No background contamination from other cells.</li> </ul>	<ul style="list-style-type: none"> <li>Discomfort similar to a blood draw</li> <li>CTC isolation dependent on targeting antibody coated on the wire.</li> </ul>
Parsortix®	ANGLE PLC, UK.	UK	CE-marked	Size-based microfluidics	<ul style="list-style-type: none"> <li>Captures heterogenous CTC populations including CTC clusters and mesenchymal cells.</li> <li>Capture and release of CTCs for downstream applications.</li> </ul>	<ul style="list-style-type: none"> <li>For research use only.</li> <li>Large volume of blood required (10 ml).</li> </ul>
ClearCell® FX	Clearbridge BioMedics, Singapore.	Singapore	CE-marked, USFDA registered	Label-free, inertial focusing microfluidics	<ul style="list-style-type: none"> <li>Captures intact and viable, heterogenous and dynamic CTC populations.</li> <li>Automated system.</li> <li>Label free.</li> <li>Post-capture downstream application compatible.</li> </ul>	<ul style="list-style-type: none"> <li>Low purity of CTCs for downstream analysis</li> </ul>

\*Prices of each CTC test varies by locations and country but ranges from approx. US\$ 200-2000. Information adapted from ref.<sup>152-156</sup>

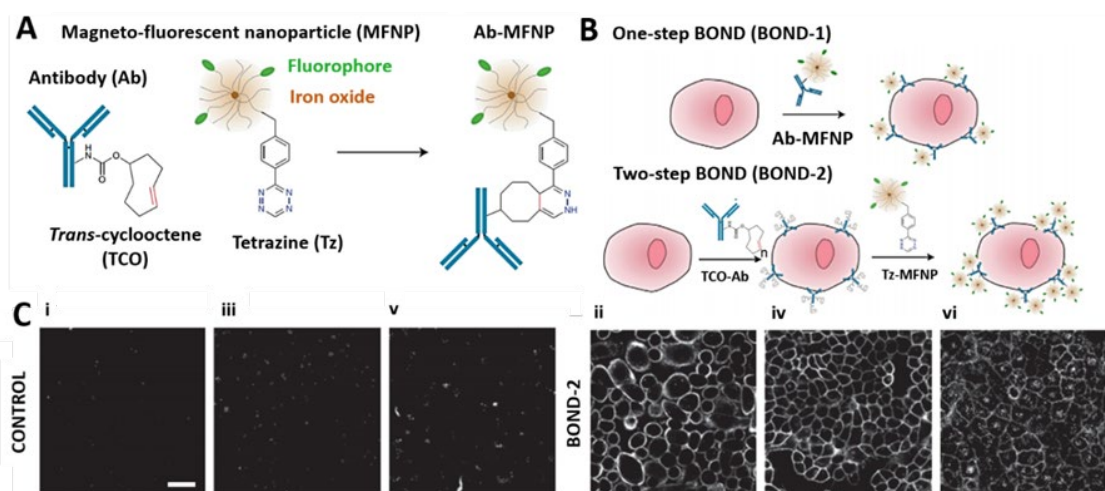


**Figure 13:** A) Bioorthogonal reaction between 1,2,4,5-tetrazine labelled fluorescent magnetic nanoparticles and trans-cyclooctene labelled antibody; B) One-step and two-step targeting of NPs to cells by BOND; C) Confocal microscopy images of labelled live cells. Control shows non-binding, BOND2 shows binding via TCO-modified control antibody (clone MOPC-21). HER2 (i,ii); EpCAM (iii,iv); EGFR (v,vi). Scale bar is 50mm. Figure adapted from ref. <sup>119</sup>

#### Magnetic polymeric nanogel system with multiple ligands for CTC capture.

Crosslinked polymer networks, especially those with three-dimensional nanogels as substrate, protect the magnetic core from nonspecific interactions with blood components and provide surface functionality for biomolecules conjugation. Moreover, nanogels using hyperbranched polymer chains may offer unique rheological traits due to multiple reactive functional groups. In addition, phase separation of such systems induced due to physicochemical stimuli such as temperature and pH results in selective biological interactions.

For example, Calderon et al. designed magnetic nanogels (MNGs) consisting of iron oxide NPs that selectively captured CTCs from a breast cancer patient's blood sample.<sup>109, 158</sup> MNGs were yielded following ultrasound-assisted thermananoprecipitation via alkyne-azide strain-promoted click chemistry, as previously developed by the same group.<sup>158</sup> Iron oxide NPs were decorated with bicyclononyne (MNP@BCN) and used as crosslinkers and anchoring points for post-synthetic PEGylation (Figure 14). Glycidyl methyl ether (GME) and ethyl glycidyl ether (EGE) were polymerized in a ring-opening polymerization process to yield thermoresponsive polymers suitable for MNGs preparation. The surface of MNGs was decorated with Tf using PEG of varying lengths to target the overexpressed Tf receptors on CTCs. The material was optimized with respect to (a) linker/spacer between the magnetic core and Tf, (b) density of linkers coupled to the MNGs, and (c) molecular weight of the thermoresponsive polymer. Comparison between PEG with various (4,8,12 units) ethylene glycol (EG) units affirmed 8 units EG as the ideal linker length with the highest CTC capturing efficiencies. In addition, the spacer to transferrin ratio also had a key role with optimal value at three linkers per Tf, attaining 81% CTC capturing efficiency with Tf<sup>+</sup> HCT116 cell lines.

#### Capture and release of CTCs using nano-magnetic substrates.

The significance of CTC release post-capture for the downstream analysis has been explained in previous sections. Lu et al. described well-established interaction, streptavidin-biotin system, decomposable immunomagnetic iron oxide beads for CTC capture and released.<sup>84, 159</sup> To evidence this, a short peptide sequence, Trp-Ser-His-Pro-Gln-Phe-Glu-Lys, Strep-tag II, was functionalized with an anti-EpCAM antibody, which was specifically coupled to Strep-Tactin coated magnetic beads (STMBs) to obtain antibody-modified STMBs. The design was finally evaluated for capturing EpCAM<sup>+</sup> A431 human epidermoid carcinoma cell lines (Figure 15).

After the magnetic separation of A431 cells, the STMB was treated with biotin. Since strep-tactin has a stronger affinity for biotin, it forces Strep-tag II derived antibody to detach from STMBs, enabling the release of A431 cells. Additionally, anti-EpCAM functionalized STMBs were used to capture CTCs from cancer patients' blood samples. The method showed 79% capture efficiency, and 70% of the CTCs isolated were released by the addition of biotin, and about 85% of the released cells remained viable. Similar chemistry was published by Bai et al. wherein EpCAM recognition peptide Pep10 (VRRDAPRFSMQGLDACGGNNCNN) was conjugated onto MNPs (~200 nm) via biotin-avidin interaction. The material successfully captured and enriched human breast cancer MCF-7 and SK-BR-3 cells, liver cancer Hep G2 cells, prostate cancer PC3 cells, for rare cell and demonstrated comparable efficiency (>90%) and purity (>93%) with anti-EpCAM coated MNPs for breast, liver and prostate cancers from spiked human blood under magnetic field.<sup>115</sup>

Zhou et al. proposed using multifunctional magnetic luminescent nanoparticles (MLNPs) for efficient capture and recovery of CTCs.<sup>116</sup> The material composition comprised of the quantum dots (QDs) (CdSs/ZnS) that were deposited on

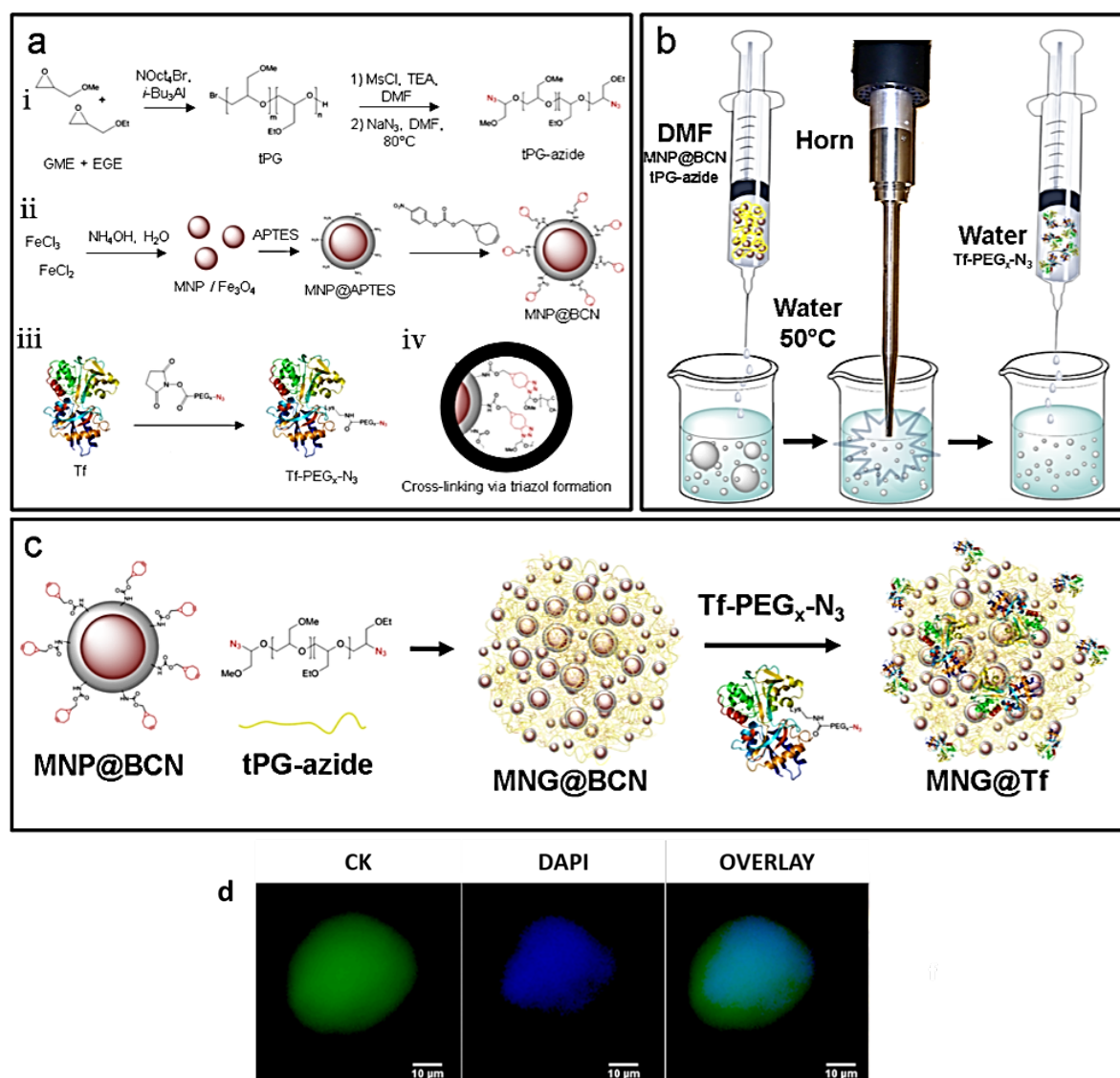


**Figure 14:** Magnetic nanogels with multiple ligands for enhanced CTC isolation. a) Synthesis of nanogel precursors, namely (i) linear thermoresponsive polyglycerol (tPG) with azide functionalities via polymerization of glycidyl methyl ether (GME) and ethyl glycidyl ether (EGE), (ii) magnetic nanoparticles functionalized with bicyclononyne (MNP@BCN), and (iii) Tf-functionalized PEG-N<sub>3</sub>. b-c) A typical procedure for the synthesis of magnetic nanogels via ultrasound-assisted thermo-nanoprecipitation. d) Representative fluorescence image of CTC captured using magnetic nanogels from breast cancer patient's blood. Captured CTC is CK (green) and DAPI (blue) positive. Figure adapted from ref.<sup>109, 157</sup>

poly(allylamine hydrochloride) coated magnet-responsive ( $\text{Fe}_3\text{O}_4$ -PAH) nanoparticles. Subsequently, PAH and hyaluronic acid (HA) layers were deposited through a facile layer by layer assembly method. The synthesized MLNPs (PAH/QD/PAH/HA) were successfully built to monitor the capture and recovery process in real-time. The surface carboxylic groups of MLNPs were functionalized with cystamine dihydrochloride 50% molar ratio (cys: carboxyl group), and the remaining carboxylic groups were PEGylated via carbodiimide chemistry. The nanoparticles were then treated with dithiothreitol (DTT) to cleave the cystamine disulfide bonds, and subsequently, the thiolated nanoparticles were grafted with N-succinimidyl-3-(2-pyridyldithio)propionate (SPDP) to generate free terminal NHS ester. Finally, the nanoparticles were decorated with anti-

EpCAM antibody. The exquisiteness of these MLNPs is that in the existence of glutathione (GSH), the disulfide bond between cys-SPDP would cleave, thereby releasing the captured CTCs. The MLNPs showed 99% capture efficiency using MCF-7 cell lines (EpCAM<sup>+</sup>). Moreover, on GSH treatment, cell viability was investigated using the Live/Dead staining method, displaying almost 100% cell release efficiency with 98% cell viability.

Xiao et al. utilized the principle advantage of deoxyribonucleic acid (DNA) aptamer and their easy cleavage by introducing a DNA complementary sequence or nuclease, to capture and release CTCs (Figure 16).<sup>115</sup> DNA aptamer, a single-stranded nucleic acid molecule that binds targets of interest in an antibody-like manner, possess several advantages over antibodies, such as shorter generation time, low manufacturing

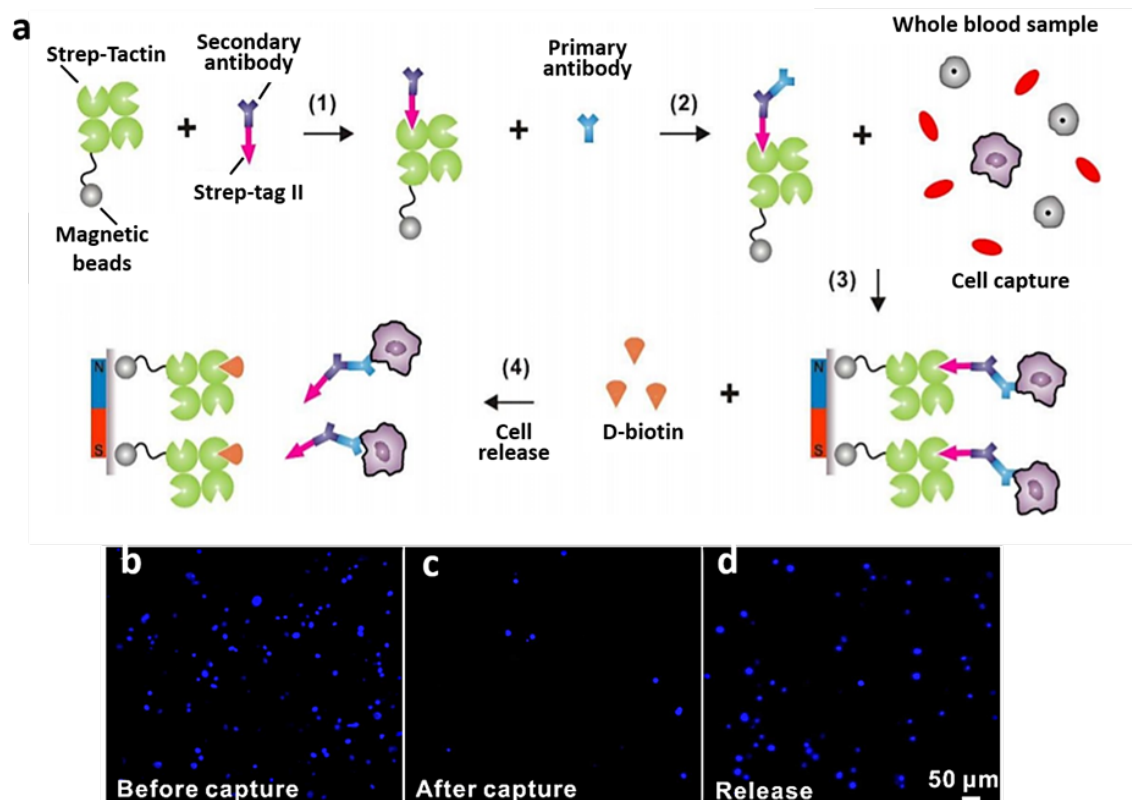


**Figure 15:** Schematics for immunomagnetic based CTC enrichment and release. a) Strep-Tactin coated magnetic beads (STMBs) for CTC capture and their biotin triggered release (1) Strep-tag II labelled Secondary Antibody (anti-mouse IgG) reacted with STMBs; (2) Anti-EpCAM, anti-EGFR or anti-HER2 interacted with IgG-STMBs for grafting antibody over IgG-STMBs; (3) Antibody grafted STMBs used to capture CTCs; (4) Biotin triggered the release of captured CTCs; Capture and release of cancer cells (b-d) Fluorescent microscopic images of SK-BR-3 cells before (b), after (c) incubation with anti-EpCAM-IgG-STMBs; Released SK-BR-3 cells (d).<sup>84</sup>

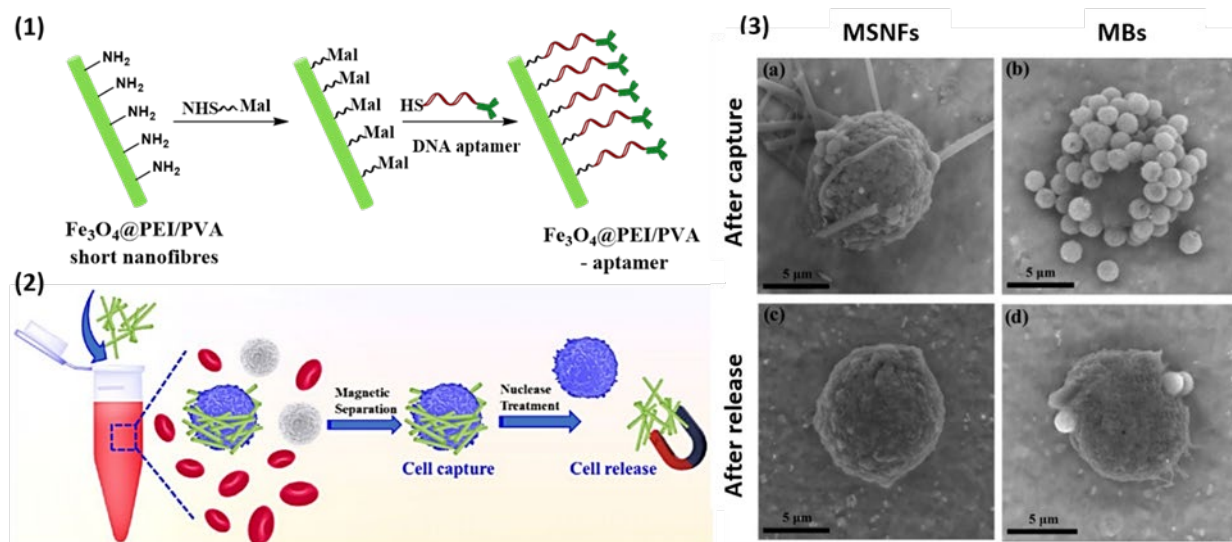


**Figure 16:** (1-2) Schematic of surface functionalization of MSNFs for capture and release of cancer cells (MCF-7); (3) SEM images of MCF-7 cells captured by (a) aptamer-MSNFs and (b) aptamer-Magnetic beads (MBs) and after cell release treatment (c) to remove the MSNFs and (d) to remove the MBs.<sup>117</sup>

costs, consistency between batches, higher modifiability, enhanced thermal stability, and enhanced target potential from ions to live animals.<sup>160</sup> The synthetic methodology of the reported material involved the preparation of polyethyleneimine (PEI)-functionalized iron nanoparticles ( $\text{Fe}_3\text{O}_4@$ PEI NPs) that were dip-coated with PEI/polyvinyl alcohol nanofibers via a blended electrospinning process to obtain magnetic short nanofibers (MSNFs). Further, these composite nanofibers ( $\text{Fe}_3\text{O}_4@$ PEI/PVA) were crosslinked with glutaraldehyde vapors for improved stability in water. Amine-functionalized MSNFs surface was then grafted with 3-(maleimido)propionic acid N-hydroxysuccinimide ester. Finally, the surface of DNA aptamer was functionalized through thiol-maleimide coupling to generate aptamer-MSNFs. The developed aptamer-MSNFs specifically captured MCF-7 (EpCAM<sup>+</sup>) cancer cells with 87% efficiency and enabled the non-destructive release of cancer cells with 91% efficiency after nuclease treatment.<sup>83</sup> Even though, aptamer-MSNFs revealed high capture efficiencies (83-94%) for various EpCAM<sup>+</sup> cancer cells (MCF-7, 88%; A549, 94%; and HepG2, 83%), quite low capture efficiency i.e. around 3.2% was observed for EpCAM<sup>-</sup> cancer cells (HeLa).

#### Micro-rockets with a propellent motion for CTC interaction and capture.

Iron oxide-based CTC capture platforms have shown great promise in isolation and enrichment of CTCs from peripheral

blood. Interestingly, the employment of another nanostructure system in combination with iron oxide nanoparticles, such as FeNP-Graphene or FeNP-CNT can further enhance the material's efficiency, selectivity, and specificity. Such a system would provide synergistic augmented multivalences and high density of functionalization units per molecules for efficient ligand-receptor interactions. For example, graphene/CNT oxide - Iron oxide NPs, is a synergistic system wherein graphene/CNT offers higher number of functionalities (free acidic group) per molecule for antibody conjugation and iron nanoparticles core would allow magnetic separation from the bulk.

In this context, Banerjee et al. described a multi-component material involving  $\text{H}_2\text{O}_2$ -driven  $\text{O}_2$  bubble-propelled micro-rockets to precisely capture CTCs.<sup>111</sup> The micro-rocket system consisted of three functional components: (i) CNTs for increasing surface area, (ii) magnetic NPs for isolation, and (iii) transferrin for specific CTC targeting. The chemical mechanism in the form of oxidation using CNTs was introduced to generate carboxylic acid functionality, followed by the loading of iron oxide NPs within the inner surface of CNTs by incubating oxidized CNTs with divalent and trivalent iron chloride salts. Finally, transferrin was functionalized on the CNT- $\text{Fe}_3\text{O}_4$  via carbodiimide chemistry (Figure 17). The self-propulsion of suspended Tf-CNT- $\text{Fe}_3\text{O}_4$  microparticles mimicked a micro-rocket due to the oxidative release of  $\text{O}_2$  in the existence of  $\text{H}_2\text{O}_2$ , with the speed of the micro-rocket being dependent on the percentage of  $\text{H}_2\text{O}_2$  concentration. This self-powered

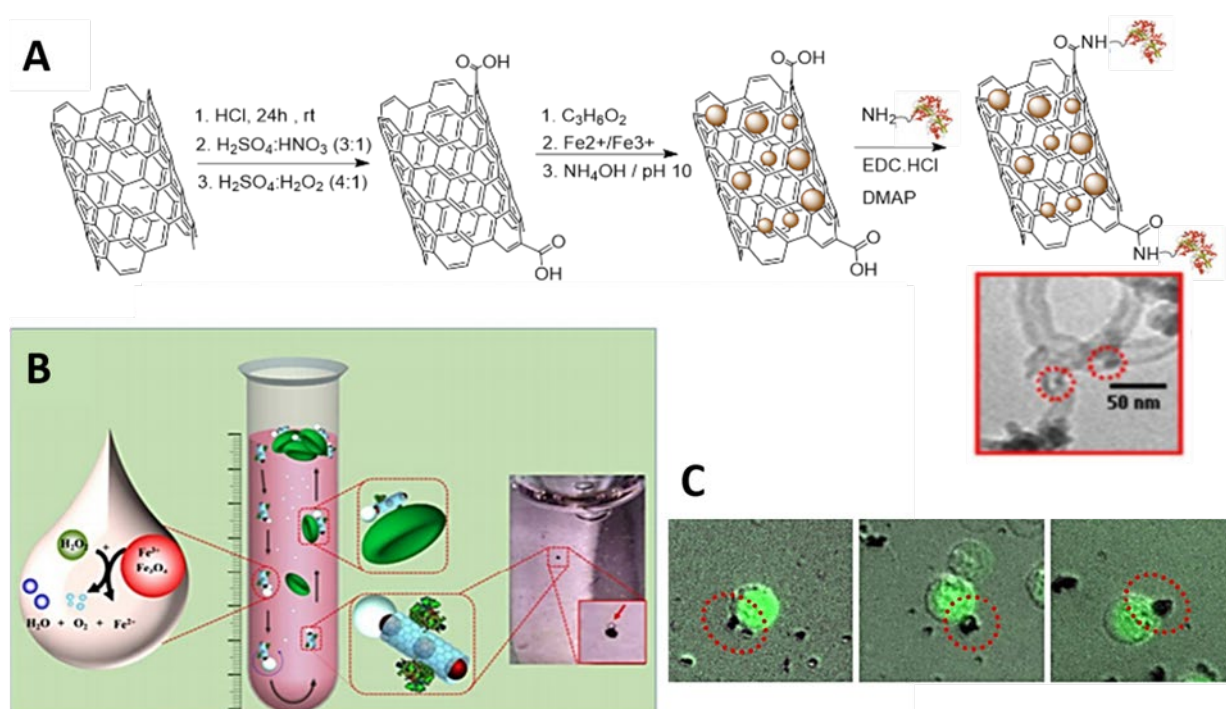


**Figure 17:** A) Tf-CNT- $\text{Fe}_3\text{O}_4$ . Inset shows TEM image of Tf- $\text{Fe}_3\text{O}_4$ -CNT system (red dotted circles indicate presence of  $\text{Fe}_3\text{O}_4$  in CNT); B) Schematic of the driving mechanism for the Tf- $\text{Fe}_3\text{O}_4$ -CNT micro-rocket. The right side inset shows the upward moving Tf- $\text{Fe}_3\text{O}_4$ -CNT micro-rocket due to the oxidative release of  $\text{O}_2$  in the existence of  $\text{H}_2\text{O}_2$ , as indicated by an arrow; C) Fluorescence image of Tf-CNT- $\text{Fe}_3\text{O}_4$  micro-rocket attached to the HCT116 cells in just 5 min. Adapted from ref.<sup>111</sup>

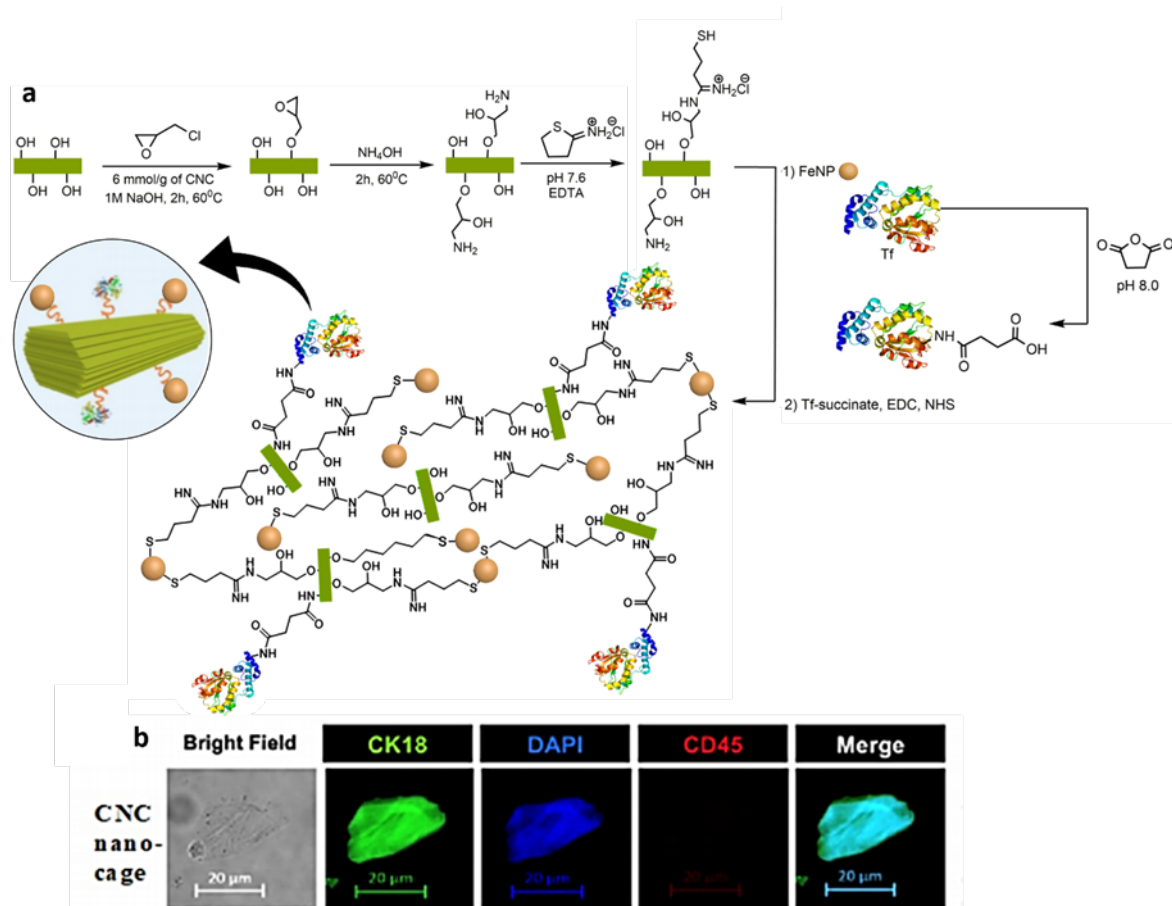


**Figure 18:** a) Synthetic scheme for conjugation of cellulose nanocages to iron nanoparticles followed by functionalization with transferrin; b) Fluorescence image of isolated CTCs by CNC nanocages from a blood sample of HNC patient. Captured cells were labelled with CK18 (green), CD45 (red), and DAPI (blue): nuclei staining. Figure adapted from ref.<sup>112</sup>

system allowed ~85% efficiency (TfR<sup>+</sup>) to capture human colorectal carcinoma (HCT) 116 cells and CTC extraction from biological fluids.

Conversely, Li et al. designed magnetic halloysite nanotubes (MHNTs) - folic acid composite to target the Folic acid (FA) receptor on cancer cells.<sup>120</sup> The MHNTs composite was synthesized by mixing HNTs with divalent and trivalent iron salts in a one-step co-precipitation method. Next, these MHNTs were functionalized with Ad-PEG-FA (Admantane-PEG-Folic acid), using carboxylated  $\beta$ -cyclodextrin (CD) as a linker, to get MHNTs@ $\beta$ -CD@Ad-PEG-FA. The material's specificity was determined by incubating MHNTs@ $\beta$ -CD@Ad-PEG-FA nanocomposite with 100,000 Skov3, Hela, or A549 cells. The peak efficiency of 95.6% (for all cell lines) was obtained compared to non-FA receptor normal HEK 293T, which showed <10% efficiency.

Recently, Quadir et al. stated water-dispersible 'nanocages' composed of cellulose nanocrystals (CNCs), covalently linked to magnetic FeNPs (Figure 18).<sup>112</sup> These systems were composed of cellulose nanocrystals (CNCs) obtained from bio-based resources. Multiple hydroxyl groups on CNCs render the molecule ideal for the multivalent conjugation of CTC-targeting ligand (Tf).<sup>161</sup> In addition, these functional groups also provide

a hydrophilic microenvironment for the captured CTCs. The native CNCs were functionalized using epichlorohydrin chemistry to generate multiple amine functional groups. Through iminothiolane-mediated immobilization of thiol groups on these amines, these authors were able to conjugate FeNPs, and succinylated transferrin. While the metal-thiol interaction was characterized by X-ray photoelectron microscopy and high-resolution TEM, the success of covalent conjugation of Tf-succinate to amine-functionalized CNC was followed by IR spectroscopy. The synthesized product was found to organize in the form of a metal 'nanocage' where the metal NPs were found to be stabilized within the CNC cross-linked matrix. The authors also observed that such a self-organized structure was magnetically active and formed stable nanoscale colloids with average particle size of  $254.0 \pm 6.0$  nm. The presence of NPs ensured that the nanocages were magnetic and thus enabled CTC capture. Tf-CNC-based nanocages were compared with clinically relevant OncoViu<sup>®</sup> platform for the CTC capturing efficiency using the blood samples of HNC patients.

Shi et al. published another chemo-specific design having multiple discrete components, including multi-functional graphene oxide quantum dots (GOQDs) and magnetic nanoplatfor for specific separation and diagnosis of

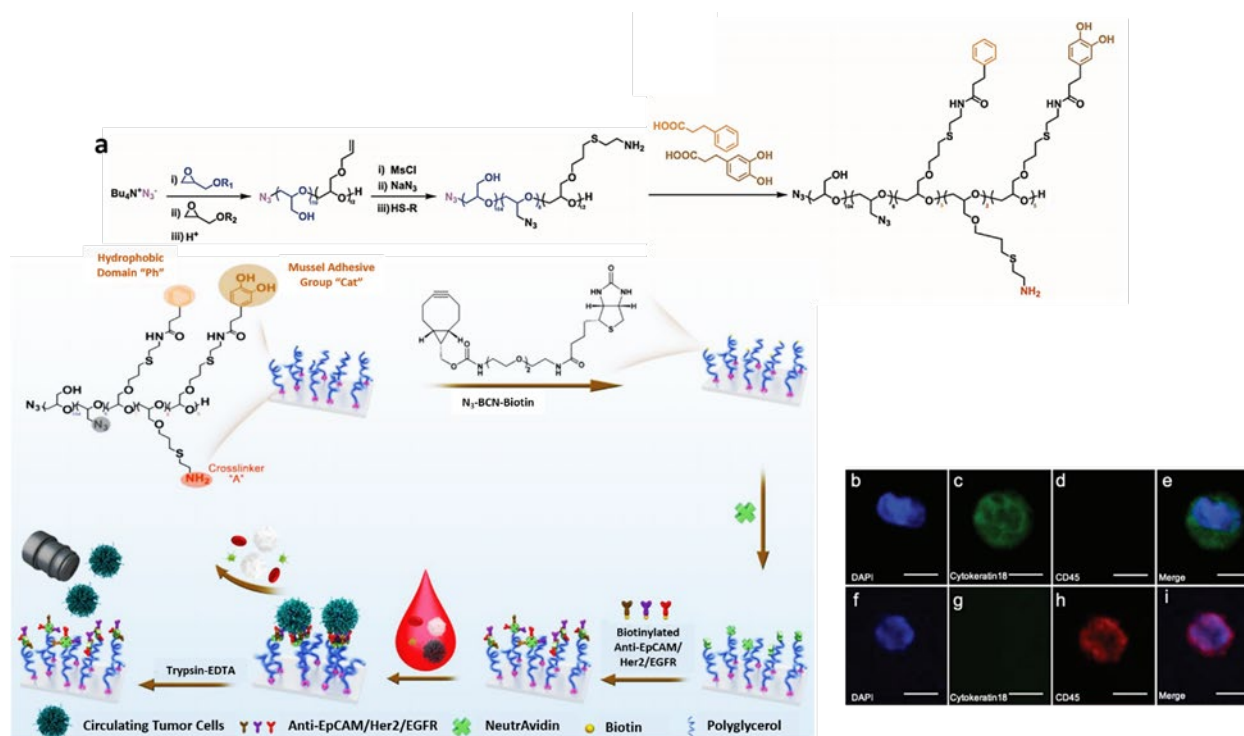


**Figure 19:** Schematic for the synthesis of polyglycerol-based copolymer used for coating  $\text{TiO}_2$  functionalized glass surface. a) Synthesis of polyglycerol-based copolymer using catechol and phenyl groups as an anchoring substrate. While the terminal azides serve as post-functionalized sites; b-i) Fluorescence image of isolated CTCs and WBCs from advanced breast cancer patients, respectively. The isolated cells stained with DAPI (blue), anti-cytokeratin18 (green), and anti-CD45 (red) respectively. Scale bar depicts 5  $\mu\text{m}$ . Figure adapted from ref.<sup>121</sup>

hepatocellular carcinoma (HCC) tumor CTCs from cancer patients' blood.<sup>162</sup> The multi-component nanosystem offered paramagnetism and multiphoton luminescence that allowed magnetic separation of enriched CTCs followed by two-photon imaging. The system comprised of GOQDs conjugated to MNPs via amine-modified PEG using carbodiimide coupling. Finally, monoclonal anti-GPC3 antibody grafted over GOQDs using EDC, NHS chemistry. Here PEG serves not only as a linker for localized spatial movement of the antibody but also prevents nonspecific interactions with blood cells. Antibody decorated GOQDs-MNPs displayed 97% capture efficiency while only GOQDs-MNPs showed only <2% efficiency.

#### Glass surface coating for multivalent CTC capture with high sensitivity.

Haag et al. established a polyglycerol-based block polymer functionalized glass surface as a bio-specific interface for CTC isolation with higher selectivity.<sup>121</sup> Titanium dioxide ( $\text{TiO}_2$ ) slides were prepared via chemical vapor deposition (CVD) of  $\text{TiO}_2$  onto clean glass cover slides.<sup>163</sup> Titanium dioxide slides were then functionalized with polyglycerol (PEG) based poly(ethoxyethyl glycidyl ether)-block-poly(allyl glycidyl ether) (PEEGE-b-PAGE) copolymer with catechol groups and phenyl groups as the anchoring substrate, which mimicked mussel adhesion (Figure 19). The terminal and side-chain azide ( $\text{N}_3$ ) groups were coupled to the cyclooctene groups of BCN-biotin via catalyst-free azide-alkyne cycloaddition reaction. The slides were then

functionalized with streptavidin and finally with biotinylated anti-EpCAM/Her2/EGFR. The clinical utility of functional surface coating was tested by capturing CTCs from the advanced breast cancer patients' blood at stage II and III. High CTC number ranging from 49 to 217 CTCs  $\text{mL}^{-1}$  were obtained in breast cancer patients. Cell lines expressing low EpCAM, i.e., the MDA-MB-231 cell and A549 cell, multivalent antibodies (anti-EpCAM, anti-Her2, and anti-EGFR) were employed to obtain improved efficiency > 90%.

### 3. Chemo-specific multi-component microfluidic system for CTC Enrichment (Flow-through System)

As noted above, CTC capture platforms delineated with iron oxide nanoparticles have shown good CTC capturing efficiency (80-100%), but their utility is limited to a small blood volume (1 to 10 mL). Moreover, the amount of antibody-conjugated iron oxide nanoparticles used per milliliter of blood is very high, and the detection process requires a complex enrichment step. Therefore, lately, the microfluidic platform has emerged extensively for CTCs' detection and isolation. They possess numerous advantages over conventional methods such as automated operation, range of sample volumes ( $10^{-9}$  mL to  $10^2$  mL), reduced target cell loss, high sensitivity, and throughput. Moreover, it functions as a single step process for sample collection, loading, isolation, and analysis, resulting in significantly reduced processing time and avoids loss of rare

CTCs for multiple experimental steps. Various materials such as glass, ceramics, metals, and polymers have been utilized to construct fluidic platforms. Among all, glass and polydimethylsiloxane (PDMS) are the most frequently employed owing to their chemical flexibility, gas permeability, biological compatibility, optical properties, rapid prototyping, and cost efficiency. Furthermore, the fluidic platform can be easily functionalized with a very low volume of reagent/targeting ligand (such as an antibody) using simple coupling reactions that can be integrated with other nanomaterials/nanotechnologies for improving capture efficiency. In the past decades, researchers have studied microfluidic-based CTC enrichment techniques by utilizing the unique properties of CTCs such as density, size, deformability, surface protein expression, etc.<sup>164-167</sup> However, below, we review the advances in chemistry employed in flow-through devices to enrich CTCs based on their surface biomarker expression.

A fluidic methodology consisting of graphene oxide (GO) nanosheets patterned over PDMS fluidic channels was adapted by Kim et al. to isolate CTCs from metastatic breast cancer patients.<sup>169</sup> The chip fabrication consisted of a silicon substrate with a flower-shaped gold pattern. The device's overall size was 24.5 mm × 60 mm × 3 mm, and the height of the PDMS microfluidic chamber was 50 μm. Firstly, phospholipid-polyethylene-glycoamine (PL-PEG-NH<sub>2</sub>) was non-covalently immobilized on GO nanosheets. Tetrabutylammonium (TBA) hydroxide was used for achieving complete exfoliation and

intercalation of the GO. Following, GO nanosheets were adsorbed onto the decorated gold surface in a microfluidic chamber. The amino group of PL-PEG-NH<sub>2</sub> on GO sheets coordinated with the patterned gold surface by electrostatic attraction.<sup>170</sup>

Additionally, N-γ-maleimidobutyryloxysuccinimide ester (GMBS) was introduced, having N-hydroxysuccinimide (NHS) esters, which further was used for reacting with the amine groups of PL-PEG-NH<sub>2</sub> on the GO, forming amide bonds. Next, thiolated NeutrAvidin was introduced in the chamber coupled to the maleimido group of GMBS on the GO sheet. Finally, biotinylated anti-EpCAM was coupled to NeutrAvidin via NeutrAvidin-biotin interaction (**Figure 20**). Incorporating GO as the substrate of the antibody conjugation chemistry allowed CTC detection from 1 mL of blood with high efficiency due to the presence of dense antibody. The unique design allowed blood processing at a flow rate of 1 mL h<sup>-1</sup> while offering surface capture of CTCs with extremely low blood cell contamination, which is essential for multiple downstream analyses at both proteomic and transcriptional levels.

The short survival and rarity of tumor cells in blood require appropriately sensitive and specific techniques to identify CTCs from among billions of other blood cells. The choice of bioconjugation method and antibody linking is critical to ensure efficient cell capture but are often poorly understood mechanisms. In a report, Andree et al. demonstrated the binding affinity constants of the EpCAM antibodies EpAb3-5, MJ-37, VU1D-9, and HO-3 by Surface Plasmon Resonance

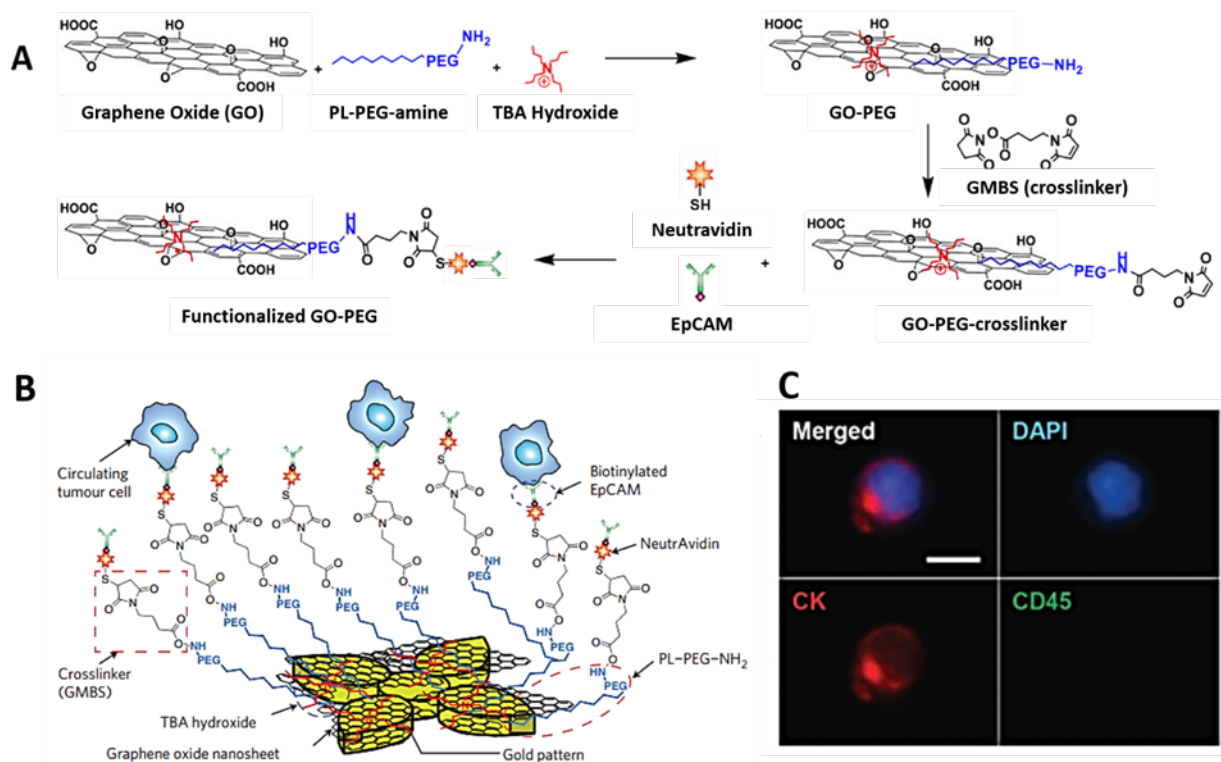


**Figure 20:** A) Synthetic Protocol for functionalizing GO-PEG on the PDMS layer conjugated to the biotinylated antibody via Neutravidin; B) Schematic of device functionalization with GO chips fixed onto a gold patterned surface; C) Representative image of isolated CTC stained for DAPI<sup>+</sup>/CK<sup>+</sup>/CD45<sup>-</sup>, showing individual and merged fluorescence channels. Adapted from ref.<sup>168</sup>

imaging (SPRi).<sup>122</sup> They reported a fluidic glass assembly by adhering two antibody-coated microscopic glass slides together. Glass surface was first functionalized with a monolayer of (3-aminopropyl)triethoxysilane (APTES). APTES functionalized glass slides were then placed in a slide holder and treated with poly(acrylic acid) (PAA), EDC, and NHS to obtain the NHS-activated PAA layer. Finally, the epitope of EpCAM antibodies EpAb3-5, VU1D-9, MJ-37, and HO-3, were treated with the NHS activated glass surface. Next, SPRi was done to compare the binding affinity of the 4 different epitopes of EpCAM antibodies. Highest binding affinity was showed by EpAb3-5 ( $K_D = 2.6E^{-11}$  M) which was comparable to the affinity of HO-3 ( $K_D = 4.0E^{-11}$  M) followed by VU1D-9 ( $K_D = 2.7E^{-10}$  M) and MJ-37 respectively ( $K_D = 2.8E^{-9}$  M). The capture efficiency of these epitopes of EpCAM antibodies was determined against breast carcinoma cell line SKBR-3 (EpCAM<sup>+</sup>) and the capture efficiency correlated with the  $K_D$  values. These results emphasize that systematic studies should be performed while choosing an antibody for such application.

Moreover, irrespective of antibody selection, its interfacial molecular organization is essential in calculating the capture efficiency. The molecules/spacer, which binds the surface of the microfluidic device to biomolecule (e.g., EpCAM antibody), plays a fundamental role in the efficiency of the microfluidic device. Unlike nanostructures, the antibodies are not dispersed in a microfluidic device but are rather fixed to the device's surface. Therefore, a longer, flexible spacer allows the movement of antibodies in the small vicinity to efficiently capture CTCs compared to a small spacer, which keeps the antibodies fixed at one place without any movement.

Yeh et al. proved the importance of linker/spacer on a substrate with CTC isolation efficiency.<sup>81</sup> Conventionally, the antibody moieties were conjugated on microfluidic surface. Consequently, the number of antibodies-antigen pairs may be restricted by the fixed number of antibody moieties per surface area underneath a cell. Employing dendrimers or polymer brushes as long flexible linkers evade the limitations of short-chain linkers by enhancing local, short-range antibody-antigen clustering.<sup>82</sup> The same group developed three different microfluidic devices where the first device involved coating antibodies via a fixed linker resulting in limited accessibility to each cell antigen. In the second device, antibodies were coated via lipid molecules in a supported lipid bilayer (SLB) with 2-dimensional lateral mobility, ensuring antibody-antigen clustering on the SLB plane. Finally, in the last device, antibodies were coated via long spacer arm dendrimer-SLB, that allowed lateral and vertical mobility for entropic favoured spatial arrangement, resulting in maximal antibody-antigen pair formation.<sup>81</sup> Incorporating the stretchable PAMAM dendrimer proved to be an excellent mediator facilitating a multivalent effect due to their capability to pre-organize/orient ligands and easily deformable polymeric chains to allow easy antibody-antigen interaction. Compared to capture by surface lipid bilayer microfluidics only, over 170% enhancement in capture efficiency for Panc-1 cells (even for low EpCAM expressing cells) was observed using PEG-PAMAM-SLB system.

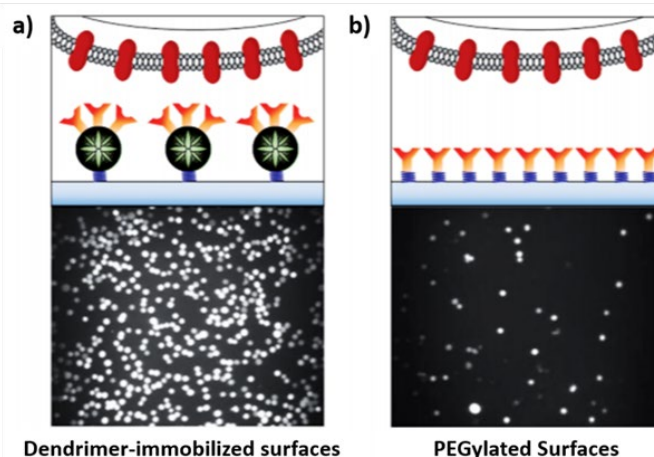


**Figure 21:** Schematics detailing the CTC capture efficiencies of dendrimer- and PEG- functionalized surfaces. Cell adhesion experiments using (a) dendrimer immobilized surfaces showing considerable improvement in CTC capture in comparison to (b) PEG immobilized surfaces. Captured tumor cells were visualized using surface plasmon resonance. Adapted from ref.<sup>82</sup>

Similar enhanced binding affinity through a multivalent binding effect using dendrimer was demonstrated by Myung and coworkers, which significantly improved the selectivity for CTC detection.<sup>82</sup> The cell capture efficiency on the anti-EpCAM functionalized dendrimer (PAMAM) / linear polymer (PEG) conjugates were tested on three cancer cell lines (MDA-MB-361, MCF-7, MDA-MB-231) under static and dynamic conditions (Figure 21). Under static conditions, an appreciably high number of cancer cells were bound on the dendrimer coated surface (up to 15.2-fold) in comparison to the PEG-coated surface. High capture efficiency was maintained underflow on the dendrimer coated surface (up to 3.7-fold) compared to the PEG-coated surface.

Liquid biopsy, the enrichment of CTCs shed from solid tumors, and their enumeration through minimally invasive approach provided an opportunity to address a long-standing oncology challenge, the real-time monitoring of tumor status and tumor heterogeneity analysis. However, even after years of effort, specific and efficient isolation, capture, and detection of CTCs with diverse phenotypes is still perplexing. To facilitate the comprehensive characterization of CTC heterogeneity, it is crucial to improve enrichment processes that meet the demand of adequate capture specificity, efficiency, and the capability to isolate cancer cells with different phenotypes. Zhao et al., while addressing the issues of tumor heterogeneity and limited availability of antibodies against tumor-specific surface markers, developed a microfluidic system using the aptamer cocktails synergistic effect.<sup>165</sup> The microfluidic chips were composed of two components, a patterned silica nanosubstrate (SiNS) and a PDMS (polydimethylsiloxane) chaotic mixer.<sup>172</sup> The SiNS was first silanized with (3-mercaptopropyl)trimethoxysilane followed by conjugation with

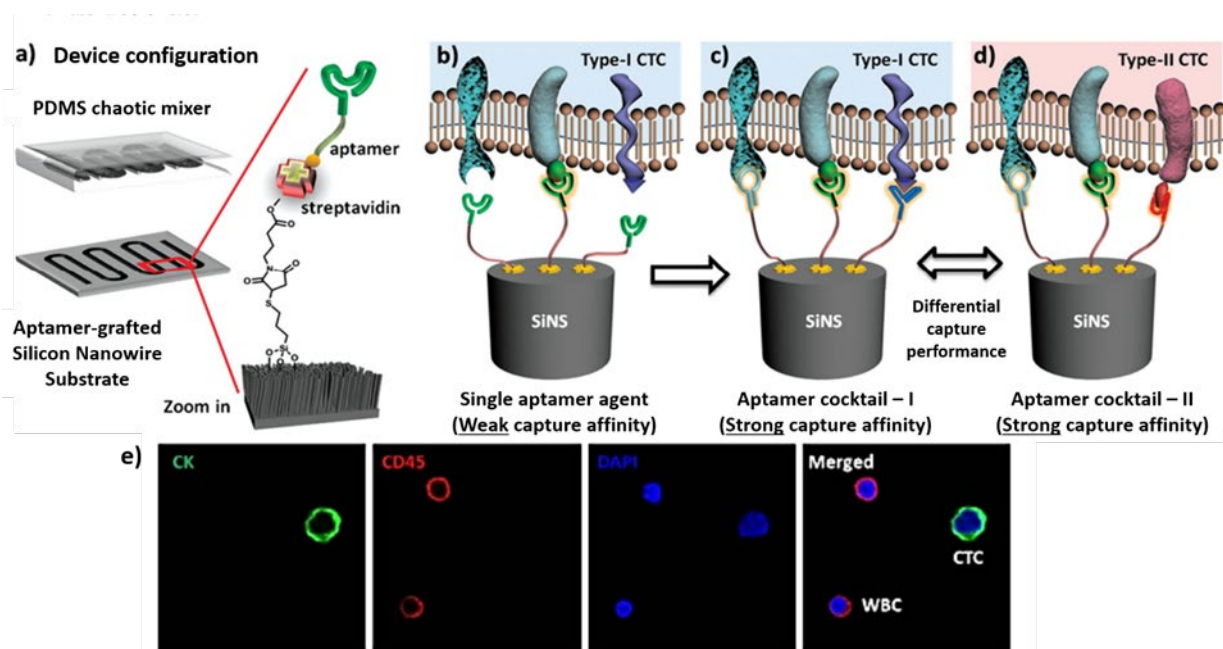


**Figure 22:** Schematics depicting CTC capture using different aptamer cocktails a) Microfluidic CTC chip incorporating aptamer grafted SiNWs laid on PDMS chaotic mixer; b) Single aptamer capture substrate showing absence of synergistic binding; c) Cocktail capture agent showing synergistic binding resulting in enhanced capture efficiency; d) Different cocktails of capturing agents for CTC subpopulation interactions; e) Fluorescence image of captured CTC and WBCs from non-small cell lung cancer patient. Adapted from ref. <sup>171</sup>

N-γ-maleimidobutyryloxysuccinimide ester (GMBS). Subsequently, streptavidin was grafted over SiNS followed by functionalization with four different biotinylated aptamers (Ap1, Ap2, Ap3, and Ap4). These aptamers target other surface markers on CTCs. Aptamer cocktails with a synergistic effect showed a better overall CTC capture efficiency than a single aptamer against NSCLC cell lines and NSCLC patients' blood samples (**Figure 22**). Head on comparison of anti-EpCAM and aptamers, and the aptamers showed almost 300% more efficiency than anti-EpCAM.

As noted microfluidic system shows greater promises for CTC isolation and enrichment, but the only major limitation of microfluidics is the reduction of capture efficiency with increasing blood flow as the fluid flow rate defines the duration of cell-antibody (protein) interaction.<sup>173</sup> Therefore, it becomes essential to maintain a low shear force in the capillary flow channel platform to maximize the attachment of CTCs, which in turn consumes time. This limits the efficiency of CTC isolation from large blood volumes.

#### Capture and Release of CTCs using a flow-through system.

Shen et al. developed NanoVelcro fluidic chip consisting of biotinylated aptamer grafted on the silicon nanowires (SiNWs) via streptavidin-biotin interaction.<sup>83</sup> The NanoVelcro chip showed >90% efficiency with NSCLC CTCs. A next-generation NanoVelcro chip was reported by the same group consisting of silica nanowires (SiNWs) covalently grafted with thermoresponsive polymer poly(N-isopropylacrylamide) (PNIPAM) and biotinylated anti-EpCAM decorated over the

nanostructure via streptavidin-biotin chemistry (**Figure 23**).<sup>174</sup> The nanostructure was capable of capturing NSCLC CTCs with high efficiency and additionally could release the immobilized CTCs upon a change in temperature as an external stimulus. Interestingly, there was an insignificant difference in CTC capture efficiency between PNIPAM grafted anti-EpCAM-SiNWs and anti-EpCAM-SiNWs.<sup>83, 174</sup>

A similar report where silicon nanostructured platform (Click Chip) was established by integrating biorthogonal ligation mediated CTC capture in combination disulfide cleavage-driven CTC release.<sup>175</sup> Dong et al. demonstrated that instead of the commonly used anti-EpCAM enriched CTC immobilization methods, click chemistry components, i.e., tetrazine (Tz) and *trans*-cyclooctene (TCO), could be grafted on cell capturing device and on CTCs, respectively. The interactions of Tz-grafted SiNWS with TCO-decorated CTCs were higher, irreversible, and insensitive to oxygen, water, and biomolecules.<sup>176</sup> This chemospecific reaction improved the CTC capture efficiency with well-preserved mRNA while reducing nonspecific immobilization of WBCs. After CTC capture, treatment with a disulfide cleavage agent (DTT) resulted in the rapid CTC release from SiNWS by cleavage of the disulfide bond enriched between Tz and SiNWS. In comparison, the Click Chips proved to be highly efficient with an overall capture efficiency of  $94 \pm 3\%$  in spite of using a lower quantity of TCO-anti-EpCAM ( $\sim 0.1$  ng) per capture study compared to with previous NanoVelcro Chips, which used 200 ng anti-EpCAM.

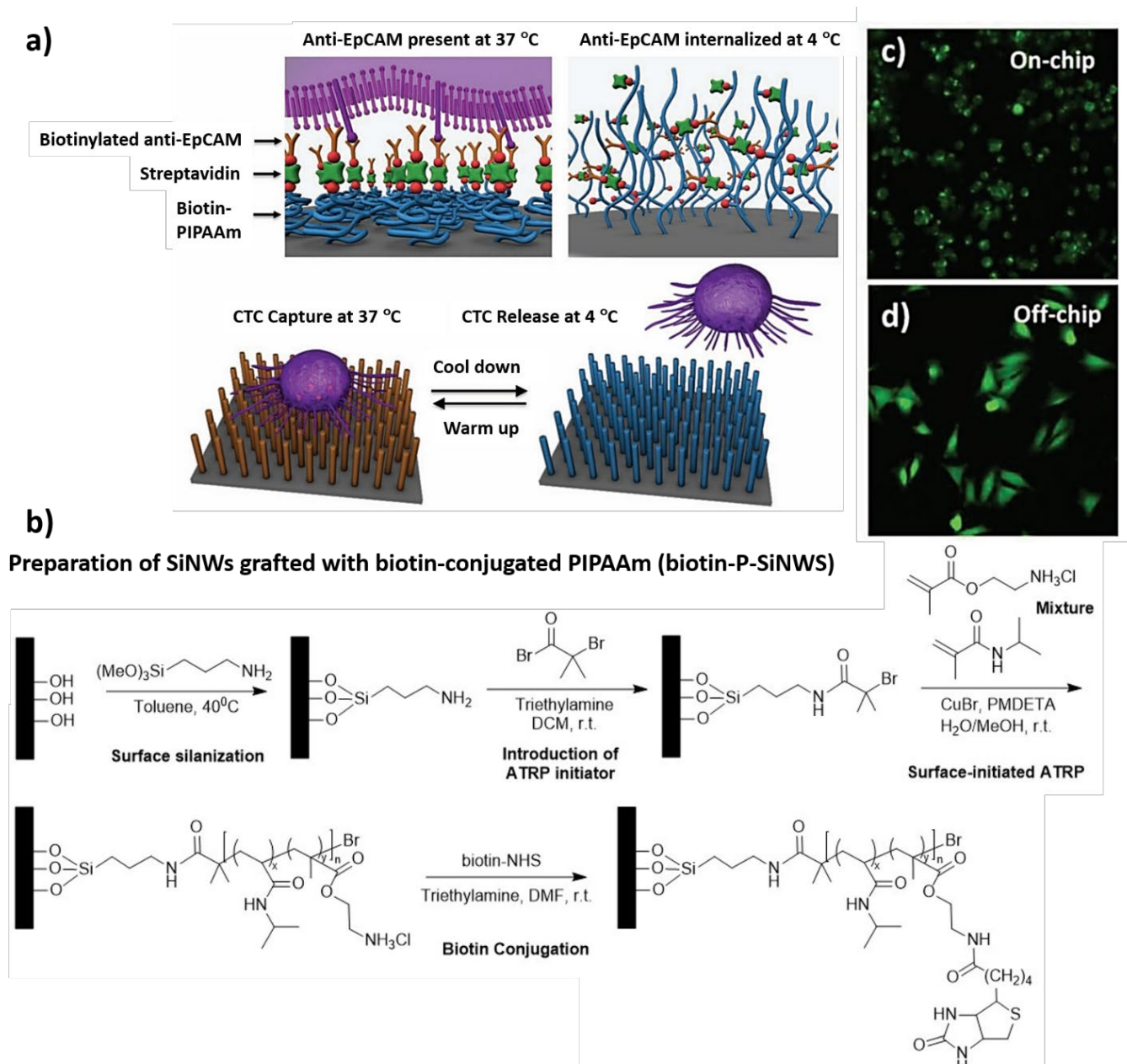


**Figure 23:** a) Conceptual illustration of capturing CTCs followed by their release upon temperature stimulation. Thermal responsiveness was conferred onto silicon nanowire substrate (SiNWS) by covalently grafting with biotin-functionalized polymer brushes (i.e., PNIPAAm); b) Conjugation reactions involved in the preparation of SiNWs grafted with biotin-conjugated PNIPAAm; c) MCF7 cells cultured after cell capture and d) successful release from anti-EpCAM coated biotin-P-SiNWS at 4 °C with retained functionality. Adapted from ref.<sup>174</sup>

#### Intravascular CTC capture (*in vivo/ ex vivo* flow-through system).

Almost all the CTC capture methodologies described above are limited to lesser blood volumes (1-100 mL); therefore, the number of captured CTCs is lower. The ability to examine larger blood volumes might increase the availability of CTCs for enumeration, which would ultimately enhance the statistical confidence of sampling for comparison and further biological characterization.<sup>177</sup> On the other hand, several *in vivo* technologies have been described to overcome the limit in using small blood volume. For example, CellCollector® involves

a structured, functionalized stainless-steel medical-grade wire that endeavours the opportunity of isolating CTCs from the peripheral blood of a cancer patient in a significantly high number, under the largest blood flow volume. The medical preparation involved a 2 μm gold layer plating deposited by galvanization, followed by a synthetic polycarboxylate hydrogel grafted to the gold layer. Finally, the carboxyl group functionalities present in the hydrogel were used for conjugation with the anti-EpCAM antibody (CD326) via carbodiimide crosslinking chemistry. The wire coated with EpCAM antibodies was introduced in the arm vein of cancer

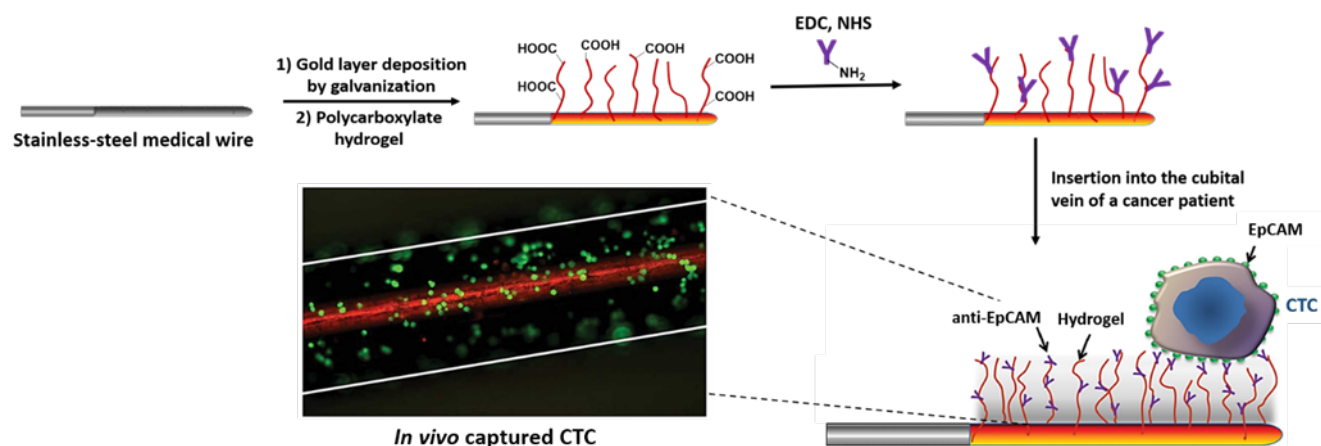


**Figure 24:** Schematic of anti-EpCAM antibody functionalized tip of medical wire. This medical wire interacts with EpCAM<sup>+</sup> CTCs, e.g., CTC of breast and lung cancer patients. Captured SK-BR-3 breast cancer cells on the wire stained with FITC-labelled antibodies (green). The white lines represent the borders of the wire. Adapted from ref.<sup>123</sup>

patients and was subjected for 30 minutes, where EpCAM<sup>+</sup> cells bind to the device (**Figure 24**). Captured CTCs were identified by staining for EpCAM, cytokeratins, and nuclear counterstain was done using Hoechst33342 with CD45 staining necessary to eliminate leukocytes. This technique has shown an elevated detection rate in several cancers, including breast, prostate, neuroendocrine, and lung.<sup>123, 178-182</sup> In fifty lung cancer patients, 185 *in vivo* applications were performed, out of which 108 wires were positive of >1 CTCs, with 20 wires showing the presence of CTC clusters.<sup>178</sup>

A different approach for *in vivo* capture of NSCLC cells by MagWIRE (magnetic wire for intravascular retrieval and enrichment) was reported by Vermesh et al.<sup>183</sup> Here, 1 mL of 2 mg mL<sup>-1</sup> antibody coated magnetic beads were infused to create an area of high magnetic nanoparticle concentration to immunomagnetically label CTCs, followed by introduction of flexible MagWIRE, composed of magnetic units of alternating

polarity. MagWIRE collects enriched magnetic nanoparticle-bound CTCs as the entire blood volume circulates over an approximate time of over 1 h. H1650 cells were captured using MagWIRE with 1 to 8% efficiency for 2,500-10,000 cells which relates to a 10-80-fold upgrading compared with 5 mL blood draw. However, this approach requires pre-injection of anti-EpCAM coated magnetic particles with alternating polarity to label CTCs, limiting its long-term usage due to possible systemic overexposure of magnetic iron nanoparticles.

Kim et al. have designed an *ex vivo* portable indwelling intravascular aphaeretic CTC monitoring tool. It can be worn for several hours by a patient to interrogate large volume of blood (**Figure 25**).<sup>184</sup> The microfluidic chips based design consist of silicon dioxide substrate patterned with a gold thin film layer bonded to PDMS structure consisting of herringbone structured microchannels that allow tumultuous mixing even at low Reynolds number. Functional GO sheets were assembled onto

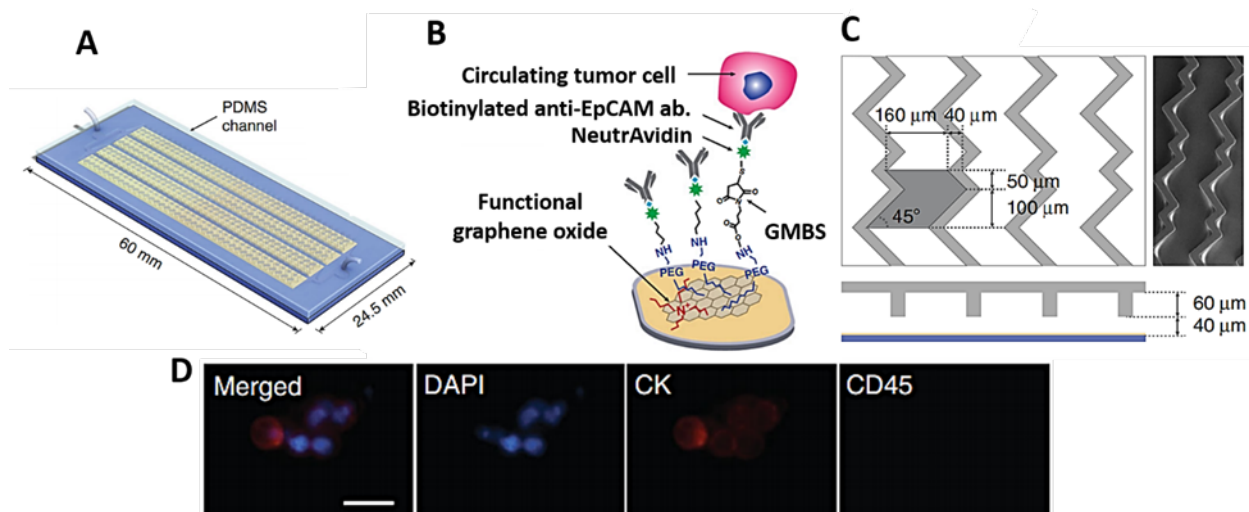


**Figure 25:** Herringbone structured graphene oxide chip for *ex vivo* capture of CTCs. A-B) Representative image of Herringbone structured graphene oxide chip and the chemistry involved between functional GO and anti-EpCAM antibody; C) Representative image of the herringbone grooved channel geometry; D) Fluorescent microscope image of MCF7 cells and clusters captured *ex vivo*. The scale bars denote 25  $\mu$ m. Adapted from ref.<sup>183</sup>

the gold layer expressing high-density EpCAM antibodies onto the substrate surface with help of PEG crosslinkers. The system has been validated first on human breast cancer MCF7 cells followed by *in vivo* animal experiments on dogs injected with non-labelled MCF7 cells. The maximal efficiency (> 90%) could be achieved at a flow rate of 1 mL/h ( $\approx 16.67 \mu\text{L}/\text{min}$ ), which dropped on increasing the flow rate. After CTC enrichment, the system returned the remaining blood to the body, and the system was capable of screening 1-2% of the whole blood over 2 h. Xie et al. and co-workers published an *in vivo* methodology to capture and downregulate colorectal CTCs, which might lead to metastasis prevention in cancer survivors after surgery.<sup>185, 186</sup> The reported system consisted of surface-functionalized PAMAM dendrimers as a scaffold to accommodate a cocktail of antibodies (anti-EpCAM and antiSlex antibodies) to capture cancer cells in harmony (HT29 colorectal cell line used as CTC model). To evaluate the capturing effects of the conjugates using HT29 cells, anti-EpCAM and antiSlex were linked to phycoerythrin (PE, orange fluorescence) and Fluorescein isothiocyanate (FITC, green fluorescence), respectively. CTCs were captured from mice blood when cancer cells and PAMAM-dual antibody conjugates were injected into the nude mice. High capture efficiency and specificity were observed with dual antibody conjugates compared to its single antibody conjugate for HT29 cells.

There still exist some caveats of the *in vivo cell* enrichment approach that includes the requirement of a long time to ensure maximal blood flows over the vein indwelling needle for CTC capture. Also, the cost of the system is high, as CTC capture is dependent on large number of antibodies.

#### 4. Discussion

This review primarily focused on advanced materials and chemo-specific designs at the nano/micrometer scale in isolating circulating tumor cells (CTCs). The development of advanced materials for next-generation, clinically relevant technologies reshapes the medical landscape, both from the clinician's and patient's perspectives. Moreover, when confronted with the burden of diseases like cancer and concomitant mortality from metastatic progression, it is prudent to emphasize the urgent requirement for timely diagnosis that can directly impact crucial prognostic and treatment decisions. To that end, considerable basic and clinical research is focused on developing future, commercially viable, diagnostic, and theranostic tools to aid in cancer disease management.

A wide range of materials from the nano to micro-meter scale have been designed and chemically tuned to offer exceptional sensitivity and selectivity for isolating rare tumorigenic cells, like CTCs, from cancer patient's peripheral blood using liquid biopsy methods, thereby providing a real-time snapshot of the disease status. This review primarily detailed the chemo-functionalities and structure-activity relationship of advanced material substrates involved in the generation of chemo-specific substrates conjugated to CTC surface tumor-specific targeting ligands. Currently, the method of choice of CTC isolation

employs highly magnetic, low nonspecific binding, colloidal magnetic particles, which are easily manipulated using an external magnetic field. Furthermore, the utility of magnetic-assisted, multi-component chemo designs involving ligand-based nanogels, cellulose systems, and micro-rockets offer CTC capture with higher efficiencies from a mixed population of nucleated cells.

The multicomponent platforms provide synergistic augmented multivalences and a high density of targeting units per molecule for efficient ligand-receptor interactions. Lately, the amount of antibody conjugated to nanoparticles used per mL of blood is extremely high, making the process expensive. In contrast, fluidic systems can be directly functionalized with a very low amount of targeting ligand and integrated with nanomaterial. Such chemo-dynamic systems allow maximal receptor-target interaction by controlling the residence time of blood containing CTCs.

Since it is clinically relevant to study molecular and functional read-outs post CTC capture, the chemo-design is equipped with linkers/targeting ligands to release CTCs without disrupting their viability and functions. Other targeting ligands that bind to the cell surface such as transferrin, aptamers, folic acid, etc. should be implemented since they offer low manufacturing costs and better thermal stabilities.

It is noteworthy that while the biological interaction between the cell surface-expressed tumor biomarker and the respective capturing moiety is not easily manipulated, the material chemistry governing the systematic synthesis of the capture substrate is subject to a high degree of control and order of chemical reactions. To that end, the choice of the chemo-specific substrates, reactive linkers, and chemical methodologies used for synthesizing CTC capture materials are crucial in ascertaining that the endpoint capture-moiety conjugated substrates are highly efficient and specific in their targeting. Furthermore, the review highlights the necessity for efficient and specific capture of CTCs and the downstream genomic advances utilized to identify, characterize, and classify the heterogenic nature of these metastatic seeds.

It is equally important to recognize that in spite of the breakthrough advances in material chemistry that make the above-mentioned technologies possible, there exists no 'one-solution-fits-all' method that offers comprehensive profiling of CTCs, due to their heterogenic nature. One reason for the limited clinical utility of CTCs is the lack of unified clinical standards in managing cancer treatments. Furthermore, liquid biopsy and CTC platforms have now been adapted for early detection, and real time monitoring of the response to treatment. Newer technologies are being clinically validated and adapted, and further the affordability of using such technologies is in sight. Each has its own applicable range and can achieve optimal performance only under certain conditions. Standardization of CTC isolation and detection parameters coupled with combinatorial and multicomponent strategies must be attempted to isolate CTCs with a greater limit of detection and high recovery rate. Further, there is a greater possibility of extracting genomic, proteomic, and artificial

intelligence-based predictive analysis that would reflect the accurate characteristics of the CTCs at a precise disease stage. The advent of such technologies will mark a turning point in cancer disease management. More importantly, while it is challenging to develop, both from the scientific as well as economic aspects, these game-changing technologies in management of cancer must be both accessible and affordable, particularly in developing countries, given that the burden of cancer affects individuals of all socio-economic strata globally.

## 5. Acknowledgments

The authors acknowledge the support from the Biotech. Ignition Grant from Biotechnology Industry Research Assistance Council (BIRAC) Department of Biotechnology (DBT), GOI, Nanobiotechnology Research Grant from DBT, and Technology Infrastructure-Department of Science and Technology (FIST-DST) and IKERBASQUE-Basque Foundation for Science. The authors thank Aravindan Vasudevan for proofreading the review.

## Conflicts of interest

There are no conflicts to declare.

## 6. References

1. L. Fusco, A. Gazzi, G. Peng, Y. Shin, S. Vranic, D. Bedognetti, F. Vitale, A. Yilmazer, X. Feng, B. Fadeel, C. Casiraghi and L. G. Delogu, *Theranostics*, 2020, **10**, 5435-5488.
2. L. Cheng, X. Wang, F. Gong, T. Liu and Z. Liu, *Advanced Materials*, 2020, **32**, 1902333.
3. G. Nagel, A. Sousa-Herves, S. Wedepohl and M. Calderón, *Theranostics*, 2020, **10**, 91-108.
4. P. Ray, M. Ferraro, R. Haag and M. Quadir, *Macromolecular Bioscience*, 2019, **19**, 1900073.
5. J. Shi, A. R. Votruba, O. C. Farokhzad and R. Langer, *Nano Letters*, 2010, **10**, 3223-3230.
6. S. Correa, K. Y. Choi, E. C. Dreaden, K. Renggli, A. Shi, L. Gu, K. E. Shopsowitz, M. A. Quadir, E. Ben-Akiva and P. T. Hammond, *Advanced Functional Materials*, 2016, **26**, 991-1003.
7. D. Gao, X. Guo, X. Zhang, S. Chen, Y. Wang, T. Chen, G. Huang, Y. Gao, Z. Tian and Z. Yang, *Materials Today Bio*, 2020, **5**, 100035.
8. M. Molina, M. Asadian-Birjand, J. Balach, J. Bergueiro, E. Miceli and M. Calderón, *Chemical Society Reviews*, 2015, **44**, 6161-6186.
9. S. S. Banerjee, G. V. Khutale, V. Khobragade, N. R. Kale, M. Pore, G. P. Chate, A. Jalota-Badwar, M. Dongare and J. J. Khandare, *Advanced Materials Interfaces*, 2017, **4**.
10. J. T. Connelly, J. P. Rolland and G. M. Whitesides, *Analytical Chemistry*, 2015, **87**, 7595-7601.
11. J. J. Khandare, S. Jayant, A. Singh, P. Chandna, Y. Wang, N. Vorsa and T. Minko, *Bioconjugate Chemistry*, 2006, **17**, 1464-1472.
12. M. Calderón, M. A. Quadir, S. K. Sharma and R. Haag, *Advanced Materials*, 2010, **22**, 190-218.
13. M. W. Kulka, I. S. Donskyi, N. Wurzler, D. Salz, Ö. Özcan, W. E. S. Unger and R. Haag, *ACS Applied Bio Materials*, 2019, **2**, 5749-5759.
14. J. J. Khandare, P. Chandna, Y. Wang, V. P. Pozharov and T. Minko, *Journal of Pharmacology and Experimental Therapeutics*, 2006, **317**, 929.
15. R. Raman and R. Langer, *Advanced Materials*, 2020, **32**, 1901969.
16. G. M. Whitesides, *Nature Biotechnology*, 2003, **21**, 1161-1165.
17. R. Duncan and M. J. Vicent, *Advanced Drug Delivery Reviews*, 2013, **65**, 60-70.
18. N.-Y. Lee, W.-C. Ko and P.-R. Hsueh, *Frontiers in pharmacology*, 2019, **10**, 1153-1153.
19. H. Khurshid, B. Friedman, B. Berwin, Y. Shi, D. B. Ness and J. B. Weaver, *AIP advances*, 2017, **7**, 056723-056723.
20. Q. Liu, Y.-C. Yeh, S. Rana, Y. Jiang, L. Guo and V. M. Rotello, *Cancer Lett*, 2013, **334**, 196-201.
21. *Nature Cancer*, 2020, **1**, 1-2.
22. F. Bray, J. Ferlay, I. Soerjomataram, R. L. Siegel, L. A. Torre and A. Jemal, *CA: A Cancer Journal for Clinicians*, 2018, **68**, 394-424.
23. L. The, *The Lancet*, 2018, **392**, 985.
24. P. Chaturvedi, A. Singh, C.-Y. Chien and S. Warnakulasuriya, *BMJ*, 2019, **365**, l2142.
25. D. Hanahan and R. A. Weinberg, *Cell*, 2000, **100**, 57-70.
26. H. Dillekås, M. S. Rogers and O. Straume, *Cancer medicine*, 2019, **8**, 5574-5576.
27. P. S. Steeg, *Nature Reviews Cancer*, 2016, **16**, 201-218.
28. D. Yao, C. Dai and S. Peng, *Molecular Cancer Research*, 2011, **9**, 1608.
29. F. Nurwidya, J. Zaini, A. C. Putra, S. Andarini, A. Hudoyo, E. Syahrudin and F. Yunus, *Chonnam Med J*, 2016, **52**, 151-158.
30. T. P. Butler and P. M. Gullino, *Cancer Research*, 1975, **35**, 512.
31. Y. S. Chang, E. di Tomaso, D. M. McDonald, R. Jones, R. K. Jain and L. L. Munn, *Proceedings of the National Academy of Sciences of the United States of America*, 2000, **97**, 14608-14613.
32. T. Lozar, K. Gersak, M. Cemazar, C. G. Kuhar and T. Jesenko, *Radiol Oncol*, 2019, **53**, 131-147.
33. J. Khandare, B. N. Qayyumi, A. Bharde, G. Aland, A. Sagare, S. Tripathi, N. Singh, S. Jayant, A. Muglikar, R. Badave, A. Vasudevan, K. Prabhash and P. Chaturvedi, *Clinical Cancer Research*, 2020, **26**, B30.
34. J. Khandare, B. Qayyumi, A. Bharde, G. Aland, S. Jayant, S. Tripathi, N. Singh, R. Badave, A. D'Souza, B. Singh, S. Arora, N. Kale, A. Vasudevan, A. Ashturkar, K. Prabhash and P. Chaturvedi, *Journal of Clinical Oncology*, 2020, **38**, e15541-e15541.
35. L. Cabel, C. Proudron, H. Gortais, D. Loirat, F. Coussy, J.-Y. Pierga and F.-C. Bidard, *International Journal of Clinical Oncology*, 2017, **22**, 421-430.
36. M. G. Krebs, R. L. Metcalf, L. Carter, G. Brady, F. H. Blackhall and C. Dive, *Nature Reviews Clinical Oncology*, 2014, **11**, 129-144.

37. [https://documents.cellsearchctc.com/pdf/e631600001/e631600001\\_EN.pdf](https://documents.cellsearchctc.com/pdf/e631600001/e631600001_EN.pdf).
38. J. Khandare, B. N. Qayyumi, A. Bharde, G. Aland, S. Jayant, S. Tripathi, N. Singh, R. Badwe, A. Souza, B. Singh, S. Arora, N. Kale, A. Vasudevan, K. Prabhaskar and P. Chaturvedi, *Cancer Research*, 2020, **80**, LB-148.
39. J. P. Thiery, *Nature Reviews Cancer*, 2002, **2**, 442-454.
40. N. Aceto, A. Bardia, D. T. Miyamoto, M. C. Donaldson, B. S. Wittner, J. A. Spencer, M. Yu, A. Pely, A. Engstrom, H. Zhu, B. W. Brannigan, R. Kapur, S. L. Stott, T. Shioda, S. Ramaswamy, D. T. Ting, C. P. Lin, M. Toner, D. A. Haber and S. Maheswaran, *Cell*, 2014, **158**, 1110-1122.
41. I. J. Fidler, *JNCI: Journal of the National Cancer Institute*, 1970, **45**, 773-782.
42. T. R. Ashworth, *Aust Med J.*, 1869, **14**, 146.
43. K. Andree, G. Dalum and L. Terstappen, *Molecular Oncology*, 2015, **10**.
44. H. K. Brown, M. Tellez-Gabriel, P.-F. Cartron, F. M. Vallette, M.-F. Heymann and D. Heymann, *Drug Discovery Today*, 2019, **24**, 763-772.
45. M. M. Ferreira, V. C. Ramani and S. S. Jeffrey, *Molecular oncology*, 2016, **10**, 374-394.
46. E. Rossi and R. Zamarchi, *Frontiers in genetics*, 2019, **10**, 958-958.
47. I. S. Batth, A. Mitra, S. Manier, I. M. Ghobrial, D. Menter, S. Kopetz and S. Li, *Annals of oncology : official journal of the European Society for Medical Oncology*, 2017, **28**, 468-477.
48. S.-m. Park, D. J. Wong, C. C. Ooi, D. M. Kurtz, O. Vermesh, A. Aalipour, S. Suh, K. L. Pian, J. J. Chabon, S. H. Lee, M. Jamali, C. Say, J. N. Carter, L. P. Lee, W. G. Kuschner, E. J. Schwartz, J. B. Shrager, J. W. Neal, H. A. Wakelee, M. Diehn, V. S. Nair, S. X. Wang and S. S. Gambhir, *Proceedings of the National Academy of Sciences*, 2016, **113**, E8379.
49. Q. Wang, L. Zhao, L. Han, X. Tuo, S. Ma, Y. Wang, X. Feng, D. Liang, C. Sun, Q. Wang, Q. Song and Q. Li, *Journal*, 2019, **15**, 21-29.
50. M. J. M. Magbanua, H. S. Rugo, D. M. Wolf, L. Hauranieh, R. Roy, P. Pendyala, E. V. Sosa, J. H. Scott, J. S. Lee, B. Pitcher, T. Hyslop, W. T. Barry, S. J. Isakoff, M. Dickler, van, L. t Veer and J. W. Park, *Clinical Cancer Research*, 2018, **24**, 1486.
51. H. Tada, H. Takahashi, Y. Kuwabara-Yokobori, M. Shino and K. Chikamatsu, *Oral oncology*, 2020, **102**, 104558.
52. S. Y. Lin, S.-C. Chang, S. Lam, R. Irene Ramos, K. Tran, S. Ohe, M. P. Salomon, A. A. S. Bhagat, C. Teck Lim, T. D. Fischer, L. J. Foshag, C. L. Boley, S. J. O'Day and D. S. B. Hoon, *Clinical chemistry*, 2020, **66**, 169-177.
53. C. Koch, A. Kuske, S. A. Joosse, G. Yigit, G. Sflomos, S. Thaler, D. J. Smit, S. Werner, K. Borgmann, S. Gärtner, P. Mossahebi Mohammadi, L. Battista, L. Cayrefourcq, J. Altmüller, G. Salinas-Riester, K. Raithatha, A. Zibat, Y. Goy, L. Ott, K. Bartkowiak, T. Z. Tan, Q. Zhou, M. R. Speicher, V. Müller, T. M. Gorges, M. Jücker, J.-P. Thiery, C. Briskin, S. Riethdorf, C. Alix-Panabières and K. Pantel, *EMBO molecular medicine*, 2020, **12**, e11908-e11908.
54. S. L. Stott, R. J. Lee, S. Nagrath, M. Yu, D. T. Miyamoto, L. Ulkus, E. J. Inserra, M. Ulman, S. Springer, Z. Nakamura, A. L. Moore, D. I. Tsukrov, M. E. Kempner, D. M. Dahl, C.-L. Wu, A. J. Iafrate, M. R. Smith, R. G. Tompkins, L. V. Sequist, M. Toner, D. A. Haber and S. Maheswaran, *Science translational medicine*, 2010, **2**, 25ra23-25ra23.
55. D. T. Miyamoto, R. J. Lee, S. L. Stott, D. T. Ting, B. S. Wittner, M. Ulman, M. E. Smas, J. B. Lord, B. W. Brannigan, J. Trautwein, N. H. Bander, C.-L. Wu, L. V. Sequist, M. R. Smith, S. Ramaswamy, M. Toner, S. Maheswaran and D. A. Haber, *Cancer Discovery*, 2012, **2**, 995.
56. K. Onidani, H. Shoji, T. Kakizaki, S. Yoshimoto, S. Okaya, N. Miura, S. Sekikawa, K. Furuta, C. T. Lim, T. Shibahara, N. Boku, K. Kato and K. Honda, *Cancer science*, 2019, **110**, 2590-2599.
57. FDA Approves New FoundationOne®Liquid CDx Companion Diagnostic Indications for Three Targeted Therapies That Treat Advanced Ovarian, Breast and Non-Small Cell Lung Cancer [news release]., <https://www.foundationmedicine.com/press-releases/d7f17f4f-ab71-4c2b-9b98-bb12df081de1>.
58. D. A. Haber and V. E. Velculescu, *Cancer discovery*, 2014, **4**, 650-661.
59. K. Yakimchuk, *Materials and Methods*, 2015, **5**.
60. L. Sorber, K. Zwaenepoel, V. Deschoolmeester, G. Roeyen, F. Lardon, C. Rolfo and P. Pauwels, *The Journal of Molecular Diagnostics*, 2017, **19**, 162-168.
61. J. Tie, Y. Wang, C. Tomasetti, L. Li, S. Springer, I. Kinde, N. Silliman, M. Tacey, H.-L. Wong, M. Christie, S. Kosmider, I. Skinner, R. Wong, M. Steel, B. Tran, J. Desai, I. Jones, A. Haydon, T. Hayes, T. J. Price, R. L. Strausberg, L. A. Diaz, Jr., N. Papadopoulos, K. W. Kinzler, B. Vogelstein and P. Gibbs, *Science translational medicine*, 2016, **8**, 346ra392-346ra392.
62. K. Pantel and C. Alix-Panabières, *Nature Reviews Clinical Oncology*, 2019, **16**, 409-424.
63. A. A. Chaudhuri, J. J. Chabon, A. F. Lovejoy, A. M. Newman, H. Stehr, T. D. Azad, M. S. Khodadoust, M. S. Esfahani, C. L. Liu, L. Zhou, F. Scherer, D. M. Kurtz, C. Say, J. N. Carter, D. J. Merriott, J. C. Dudley, M. S. Binkley, L. Modlin, S. K. Padda, M. F. Gensheimer, R. B. West, J. B. Shrager, J. W. Neal, H. A. Wakelee, B. W. Loo, Jr., A. A. Alizadeh and M. Diehn, *Cancer discovery*, 2017, **7**, 1394-1403.
64. Y.-Q. Li, B. K. Chandran, C. T. Lim and X. Chen, *Advanced Science*, 2015, **2**, 1500118.
65. Y. Ming, Y. Li, H. Xing, M. Luo, Z. Li, J. Chen, J. Mo and S. Shi, *Frontiers in Pharmacology*, 2017, **8**, 35.
66. S. Bhana, Y. Wang and X. Huang, *Nanomedicine (London, England)*, 2015, **10**, 1973-1990.
67. D. Nordmeyer, P. Stumpf, D. Gröger, A. Hofmann, S. Enders, S. B. Riese, J. Dervede, M. Taupitz, U. Rauch, R. Haag, E. Rühl and C. Graf, *Nanoscale*, 2014, **6**, 9646-9654.
68. S. Kumar and S. H. Parekh, *Communications Chemistry*, 2020, **3**, 8.
69. C. Ge, J. Du, L. Zhao, L. Wang, Y. Liu, D. Li, Y. Yang, R. Zhou, Y. Zhao, Z. Chai and C. Chen, *Proceedings of the National Academy of Sciences of the United States of America*, 2011, **108**, 16968-16973.
70. E. Fleige, M. A. Quadir and R. Haag, *Advanced Drug Delivery Reviews*, 2012, **64**, 866-884.
71. D. Sun, Z. Chen, M. Wu and Y. Zhang, *Nanotheranostics*, 2017, **1**, 389-402.
72. J. Cheng, Y. Liu, Y. Zhao, L. Zhang, L. Zhang, H. Mao and C. Huang, *Micromachines*, 2020, **11**, 774.

73. Z. Li and G.-Y. Chen, *Nanomaterials (Basel, Switzerland)*, 2018, **8**, 278.
74. G. Pereira, C. A. P. Monteiro, G. M. Albuquerque, M. I. A. Pereira, M. P. Cabrera, P. E. Cabral Filho, G. A. L. Pereira, A. Fontesa and B. S. Santos, *Journal of the Brazilian Chemical Society*, 2019, **30**, 2536-2561.
75. Y. Wan, Y. Liu, P. B. Allen, W. Asghar, M. A. I. Mahmood, J. Tan, H. Duhon, Y.-t. Kim, A. D. Ellington and S. M. Iqbal, *Lab Chip*, 2012, **12**, 4693-4701.
76. J. Wang, M. Muto, R. Yatabe, T. Onodera, M. Tanaka, M. Okochi and K. Toko, *Sensors (Basel, Switzerland)*, 2017, **17**, 2249.
77. M. Abdolahi, D. Shahbazi-Gahrouei, S. Laurent, C. Sermeus, F. Firozian, B. J. Allen, S. Boutry and R. N. Muller, *Contrast Media & Molecular Imaging*, 2013, **8**, 175-184.
78. K. E. Fischer, B. J. Alemán, S. L. Tao, R. H. Daniels, E. M. Li, M. D. Büngrer, G. Nagaraj, P. Singh, A. Zettl and T. A. Desai, *Nano Letters*, 2009, **9**, 716-720.
79. A. S. G. Curtis and M. Varde, *JNCI: Journal of the National Cancer Institute*, 1964, **33**, 15-26.
80. W. F. Liu and C. S. Chen, *Advanced drug delivery reviews*, 2007, **59**, 1319-1328.
81. P.-Y. Yeh, Y.-R. Chen, C.-F. Wang and Y.-C. Chang, *Biomacromolecules*, 2018, **19**, 426-437.
82. J. H. Myung, K. A. Gajjar, J. Saric, D. T. Eddington and S. Hong, *Angewandte Chemie (International ed. in English)*, 2011, **50**, 11769-11772.
83. Q. Shen, L. Xu, L. Zhao, D. Wu, Y. Fan, Y. Zhou, W.-H. OuYang, X. Xu, Z. Zhang, M. Song, T. Lee, M. A. Garcia, B. Xiong, S. Hou, H.-R. Tseng and X. Fang, *Advanced Materials*, 2013, **25**, 2368-2373.
84. N.-N. Lu, M. Xie, J. Wang, S.-W. Lv, J.-S. Yi, W.-G. Dong and W.-H. Huang, *ACS Applied Materials & Interfaces*, 2015, **7**, 8817-8826.
85. N. Sun, M. Liu, W. Jine, W. Zhili, X. Li, B. Jiang and R. Pei, *Small*, 2016, **12**.
86. P. Ding, Z. Wang, Z. Wu, W. Zhu, L. Liu, N. Sun and R. Pei, *Journal of Materials Chemistry B*, 2020, **8**, 3408-3422.
87. L. Wu, L. Zhu, M. Huang, J. Song, H. Zhang, Y. Song, W. Wang and C. Yang, *TrAC Trends in Analytical Chemistry*, 2019, **117**, 69-77.
88. Y. Song, Z. Zhu, Y. An, W. Zhang, H. Zhang, D. Liu, C. Yu, W. Duan and C. J. Yang, *Analytical Chemistry*, 2013, **85**, 4141-4149.
89. D.-L. Wang, Y.-L. Song, Z. Zhu, X.-L. Li, Y. Zou, H.-T. Yang, J.-J. Wang, R.-J. Pan, C. Yang and D.-Z. Kang, *Biochemical and Biophysical Research Communications*, 2014, **453**.
90. D. Shangquan, Y. Li, Z. Tang, Z. C. Cao, H. W. Chen, P. Mallikaratchy, K. Sefah, C. J. Yang and W. Tan, *Proceedings of the National Academy of Sciences of the United States of America*, 2006, **103**, 11838-11843.
91. C. S. M. Ferreira, C. S. Matthews and S. Missailidis, *Tumor Biology*, 2006, **27**, 289-301.
92. C. Raimondi, C. Nicolazzo and A. Gradilone, *Chinese journal of cancer research = Chung-kuo yen cheng yen chiu*, 2015, **27**, 461-470.
93. U. Schnell, V. Cirulli and B. N. G. Giepmans, *Biochimica et Biophysica Acta (BBA) - Biomembranes*, 2013, **1828**, 1989-2001.
94. Z. Eslami-S, L. E. Cortés-Hernández and C. Alix-Panabières, *Cells*, 2020, **9**, 1836.
95. G. Spizzo, P. Obrist, C. Ensinger, I. Theurl, M. Dünser, A. Ramoni, E. Gunsilius, G. Eibl, G. Mikuz and G. Gastl, *International Journal of Cancer*, 2002, **98**, 883-888.
96. M. Varga, P. Obrist, S. Schneeberger, G. Mühlmann, C. Felgel-Farnholz, D. Fong, M. Zitt, T. Brunhuber, G. Schäfer, G. Gastl and G. Spizzo, *Clinical Cancer Research*, 2004, **10**, 3131.
97. P. Scheunemann, N. H. Stoecklein, A. Rehders, M. Bidde, S. Metz, M. Peiper, C. F. Eisenberger, J. Schulte Am Esch, W. T. Knoefel and S. B. Hosch, *Langenbeck's archives of surgery*, 2008, **393**, 359-365.
98. *United States Pat.*, US6365362B1, 1999.
99. *United States Pat.*, US6623982B1, 1999.
100. D. L. Adams, S. Stefansson, C. Haudenschild, S. S. Martin, M. Charpentier, S. Chumsri, M. Cristofanilli, C.-M. Tang and R. K. Alpaugh, *Cytometry Part A*, 2015, **87**, 137-144.
101. H. Wang, N. H. Stoecklein, P. P. Lin and O. Gires, *Oncotarget*, 2017, **8**, 1884-1912.
102. M. Zeisberg and E. G. Neilson, *The Journal of clinical investigation*, 2009, **119**, 1429-1437.
103. S. Ménard, S. M. Pupa, M. Campiglio and E. Tagliabue, *Oncogene*, 2003, **22**, 6570-6578.
104. J. Peng, Q. Zhao, W. Zheng, W. Li, P. Li, L. Zhu, X. Liu, B. Shao, H. Li, C. Wang and Y. Yang, *ACS Applied Materials & Interfaces*, 2017, **9**, 18423-18428.
105. M. M. Moasser, *Oncogene*, 2007, **26**, 6469-6487.
106. L. Nie, F. Li, X. Huang, Z. P. Aguilar, Y. A. Wang, Y. Xiong, F. Fu and H. Xu, *ACS Applied Materials & Interfaces*, 2018, **10**, 14055-14062.
107. L. E. Kelemen, *International Journal of Cancer*, 2006, **119**, 243-250.
108. T. R. Daniels, T. Delgado, J. A. Rodriguez, G. Helguera and M. L. Penichet, *Clinical Immunology*, 2006, **121**, 144-158.
109. C. Biglione, J. Bergueiro, M. Asadian-Birjand, C. Weise, V. Khobragade, G. Chate, M. Dongare, J. Khandare, M. C. Strumia and M. Calderón, *Polymers (Basel)*, 2018, **10**, 174.
110. S. S. Banerjee, A. Jalota-Badwar, S. D. Satavalekar, S. G. Bhansali, N. D. Aher, R. R. Mascarenhas, D. Paul, S. Sharma and J. J. Khandare, *Advanced Healthcare Materials*, 2013, **2**, 800-805.
111. S. S. Banerjee, A. Jalota-Badwar, K. R. Zope, K. J. Todkar, R. R. Mascarenhas, G. P. Chate, G. V. Khutale, A. Bharde, M. Calderon and J. J. Khandare, *Nanoscale*, 2015, **7**, 8684-8688.
112. R. S. Hazra, N. Kale, G. Aland, B. Qayyumi, D. Mitra, L. Jiang, D. Bajwa, J. Khandare, P. Chaturvedi and M. Qadir, *Scientific Reports*, 2020, **10**, 10010.
113. S. S. Banerjee, G. V. Khutale, V. Khobragade, N. R. Kale, M. Pore, G. P. Chate, A. Jalota-Badwar, M. Dongare and J. J. Khandare, *Advanced Materials Interfaces*, 2017, **4**, 1600934.
114. C. Ding, C. Zhang, X. Yin, X. Cao, M. Cai and Y. Xian, *Analytical Chemistry*, 2018, **90**, 6702-6709.
115. L. Bai, Y. Du, J. Peng, Y. Liu, Y. Wang, Y. Yang and C. Wang, *J. Mater. Chem. B*, 2014, **2**.
116. X. Zhou, B. Luo, K. Kang, S. Ma, X. Sun, F. Lan, Q. Yi and Y. Wu, *Journal of Materials Chemistry B*, 2019, **7**, 393-400.

117. Y. Xiao, L. Lin, M. Shen and X. Shi, *Bioconjugate Chemistry*, 2020, **31**, 130-138.
118. J. H. Myung, K. A. Gajjar, J. Saric, D. T. Eddington and S. Hong, *Angewandte Chemie International Edition*, 2011, **50**, 11769-11772.
119. J. B. Haun, N. K. Devaraj, S. A. Hilderbrand, H. Lee and R. Weissleder, *Nature Nanotechnology*, 2010, **5**, 660-665.
120. X. Li, J. Chen, H. Liu, Z. Deng, J. Li, T. Ren, L. Huang, W. Chen, Y. Yang and S. Zhong, *Colloids and Surfaces B: Biointerfaces*, 2019, **181**, 379-388.
121. J. Chen, L. Yu, Y. Li, J. L. Cuellar-Camacho, Y. Chai, D. Li, Y. Li, H. Liu, L. Ou, W. Li and R. Haag, *Advanced Functional Materials*, 2019, **29**, 1808961.
122. K. C. Andree, A. M. C. Barradas, A. T. Nguyen, A. Mentink, I. Stojanovic, J. Baggerman, J. van Dalum, C. J. M. van Rijn and L. W. M. M. Terstappen, *ACS Applied Materials & Interfaces*, 2016, **8**, 14349-14356.
123. N. Saucedo-Zeni, S. Mewes, R. Niestroj, L. Gasiorowski, D. Murawa, P. Nowaczyk, T. Tomasi, E. Weber, G. Dworacki, N. G. Morgenthaler, H. Jansen, C. Propping, K. Sterzynska, W. Dyszkiewicz, M. Zabel, M. Kiechle, U. Reuning, M. Schmitt and K. Lücke, *International journal of oncology*, 2012, **41**, 1241-1250.
124. S. Kim, K.-R. Shin and B.-T. Zhang, *Molecular immunocomputing with application to alphabetical pattern recognition mimics the characterization of ABO blood type*, 2004.
125. S. Riethdorf, L. O'Flaherty, C. Hille and K. Pantel, *Advanced Drug Delivery Reviews*, 2018, **125**, 102-121.
126. R. Massart, *IEEE Transactions on Magnetics*, 1981, **17**, 1247-1248.
127. J. Lee, T. Isobe and M. Senna, *Colloids and Surfaces A: Physicochemical and Engineering Aspects*, 1996, **109**, 121-127.
128. S.-J. Lee, J.-R. Jeong, S. Shin, J.-C. Kim and J.-D. Kim, *Journal of Magnetism and Magnetic Materials*, 2004, **2829050**.
129. S. Sun and H. Zeng, *Journal of the American Chemical Society*, 2002, **124**, 8204-8205.
130. Z. Li, H. Chen, H. Bao and M. Gao, *Chemistry of Materials*, 2004, **16**.
131. J. Rockenberger, E. C. Scher and A. P. Alivisatos, *Journal of the American Chemical Society*, 1999, **121**, 11595-11596.
132. K. S. Suslick, M. Fang and T. Hyeon, *Journal of the American Chemical Society*, 1996, **118**, 11960-11961.
133. S. Yu and G. M. Chow, *Journal of nanoscience and nanotechnology*, 2006, **6**, 2135-2140.
134. Z. Dai, F. Meiser and H. Möhwald, *Journal of Colloid and Interface Science*, 2005, **288**, 298-300.
135. T. González-Carreño, M. P. Morales, M. Gracia and C. J. Serna, *Materials Letters*, 1993, **18**, 151-155.
136. S. Veintemillas-Verdaguer, M. P. Morales and C. J. Serna, *Materials Letters*, 1998, **35**, 227-231.
137. M. P. Morales, O. Bomati-Miguel, R. Pérez de Alejo, J. Ruiz-Cabello, S. Veintemillas-Verdaguer and K. O'Grady, *Journal of Magnetism and Magnetic Materials*, 2003, **266**, 102-109.
138. T. Hyeon, *Chemical Communications*, 2003, DOI: 10.1039/B207789B, 927-934.
139. J. Wang, J. Sun, Q. Sun and Q. Chen, *Materials Research Bulletin*, 2003, **38**, 1113-1118.
140. Y.-h. Zheng, Y. Cheng, F. Bao and Y.-s. Wang, *Materials Research Bulletin*, 2006, **41**, 525-529.
141. B. Mao, Z. Kang, E. Wang, S. Lian, L. Gao, C. Tian and C. Wang, *Materials Research Bulletin*, 2006, **41**, 2226-2231.
142. J. G. Parsons, C. Luna, C. E. Botez, J. Elizalde and J. L. Gardea-Torresdey, *Journal of Physics and Chemistry of Solids*, 2009, **70**, 555-560.
143. F. Jiang, C. Wang, Y. Fu and R.-C. Liu, *Journal of Alloys and Compounds - J ALLOYS COMPOUNDS*, 2010, **503**.
144. *United States Pat.*, US 6,365,362 B1, 1999.
145. E. Racila, D. Euhus, A. J. Weiss, C. Rao, J. McConnell, L. W. Terstappen and J. W. Uhr, *Proc Natl Acad Sci U S A*, 1998, **95**, 4589-4594.
146. F. Herranz, B. Salinas, H. Groult, J. Pellico, A. V. Lechuga-Vieco, R. Bhavesh and J. Ruiz-Cabello, *Nanomaterials (Basel, Switzerland)*, 2014, **4**, 408-438.
147. *Europe Pat.*, 3259598, 2017.
148. L. M. Millner, M. W. Linder and R. Valdes, Jr., *Annals of clinical and laboratory science*, 2013, **43**, 295-304.
149. Z. Shen, A. Wu and X. Chen, *Chemical Society reviews*, 2017, **46**, 2038-2056.
150. L. Muínelo-Romay, M. Vieito, A. Abalo, M. A. Nocelo, F. Barón, U. Anido, E. Brozos, F. Vázquez, S. Aguin, M. Abal and R. L. López, *Cancers*, 2014, **6**, 153-165.
151. X.-X. Jie, X.-Y. Zhang and C.-J. Xu, *Oncotarget*, 2017, **8**, 81558-81571.
152. <https://www.cellsearchctc.com/>.
153. <https://oncodiscover.com/>.
154. <https://www.qiagen.com/us/product-categories/diagnostics-and-clinical-research/oncology/circulating-tumor-cells/>.
155. <https://www.isetbyrarecells.com/en/>.
156. <https://gilupi.com/gilupi-gilupi-cellcollector/>.
157. M. Asadian-Birjand, C. Biglione, J. Bergueiro, A. Cappelletti, C. Rahane, G. Chate, J. Khandare, B. Klemke, M. Strumia and M. Calderon, *Macromolecular rapid communications*, 2015, **37**.
158. M. Giubudagian, M. Asadian-Birjand, D. Steinhilber, K. Achazi, M. Molina and M. Calderón, *Polymer Chemistry*, 2014, **5**, 6909-6913.
159. C. E. Chivers, A. L. Koner, E. D. Lowe and M. Howarth, *The Biochemical journal*, 2011, **435**, 55-63.
160. Y. Zhang, B. S. Lai and M. Juhas, *Molecules*, 2019, **24**, 941.
161. V. Incani, C. Danumah and Y. Boluk, *Cellulose*, 2013, **20**, 191-200.
162. Y. Shi, A. Pramanik, C. Tchounwou, F. Pedraza, R. A. Crouch, S. R. Chavva, A. Vangara, S. S. Sinha, S. Jones, D. Sardar, C. Hawker and P. C. Ray, *ACS Applied Materials & Interfaces*, 2015, **7**, 10935-10943.
163. C. Garlisi and G. Palmisano, *Applied Surface Science*, 2017, **420**, 83-93.
164. R. Gertler, R. Rosenberg, K. Fuehrer, M. Dahm, H. Nekarda and J. R. Siewert, *Recent results in cancer research*.

- Fortschritte der Krebsforschung. Progres dans les recherches sur le cancer*, 2003, **162**, 149-155.
165. S. Ribeiro-Samy, M. I. Oliveira, T. Pereira-Veiga, L. Muinelto-Romay, S. Carvalho, J. Gaspar, P. P. Freitas, R. López-López, C. Costa and L. Diéguez, *Scientific Reports*, 2019, **9**, 8032.
166. E. Park, C. Jin, Q. Guo, R. Ang, S. Duffy, K. Matthews, A. Azad, H. Abdi, T. Todenhöfer, J. Bazov, K. Chi, P. Black and H. Ma, *Small (Weinheim an der Bergstrasse, Germany)*, 2016, **12**.
167. S. Riethdorf, H. Fritsche, V. Müller, T. Rau, C. Schindlbeck, B. Rack, W. Janni, C. Coith, K. Beck, F. Jänicke, S. Jackson, T. Gornet, M. Cristofanilli and K. Pantel, *Clinical Cancer Research*, 2007, **13**, 920.
168. H. J. Yoon, T. H. Kim, Z. Zhang, E. Azizi, T. M. Pham, C. Paoletti, J. Lin, N. Ramnath, M. S. Wicha, D. F. Hayes, D. M. Simeone and S. Nagrath, *Nature Nanotechnology*, 2013, **8**, 735-741.
169. T. H. Kim, H. J. Yoon, S. Fouladdel, Y. Wang, M. Kozminsky, M. L. Burness, C. Paoletti, L. Zhao, E. Azizi, M. S. Wicha and S. Nagrath, *Advanced Biosystems*, 2019, **3**, 1800278.
170. H. Wang, X. Wang, X. Li and H. Dai, *Nano Research*, 2009, **2**, 336-342.
171. L. Zhao, C. Tang, L. Xu, Z. Zhang, X. Li, H. Hu, S. Cheng, W. Zhou, M. Huang, A. Fong, B. Liu, H.-R. Tseng, H. Gao, Y. Liu and X. Fang, *Small (Weinheim an der Bergstrasse, Germany)*, 2016, **12**, 1072-1081.
172. S. Wang, K. Liu, J. Liu, Z. T. F. Yu, X. Xu, L. Zhao, T. Lee, E. K. Lee, J. Reiss, Y.-K. Lee, L. W. K. Chung, J. Huang, M. Rettig, D. Seligson, K. N. Duraiswamy, C. K. F. Shen and H.-R. Tseng, *Angewandte Chemie International Edition*, 2011, **50**, 3084-3088.
173. S. Nagrath, L. V. Sequist, S. Maheswaran, D. W. Bell, D. Irimia, L. Ullkus, M. R. Smith, E. L. Kwak, S. Digumarthy, A. Muzikansky, P. Ryan, U. J. Balis, R. G. Tompkins, D. A. Haber and M. Toner, *Nature*, 2007, **450**, 1235-1239.
174. S. Hou, H. Zhao, L. Zhao, Q. Shen, K. S. Wei, D. Y. Suh, A. Nakao, M. A. Garcia, M. Song, T. Lee, B. Xiong, S.-C. Luo, H.-R. Tseng and H.-h. Yu, *Advanced Materials*, 2013, **25**, 1547-1551.
175. J. Dong, Y. J. Jan, J. Cheng, R. Y. Zhang, M. Meng, M. Smalley, P.-J. Chen, X. Tang, P. Tseng, L. Bao, T.-Y. Huang, D. Zhou, Y. Liu, X. Chai, H. Zhang, A. Zhou, V. G. Agopian, E. M. Posadas, J.-J. Shyue, S. J. Jonas, P. S. Weiss, M. Li, G. Zheng, H.-H. Yu, M. Zhao, H.-R. Tseng and Y. Zhu, *Science advances*, 2019, **5**, eaav9186-eaav9186.
176. M. L. Blackman, M. Royzen and J. M. Fox, *Journal of the American Chemical Society*, 2008, **130**, 13518-13519.
177. A. L. Allan and M. Keeney, *Journal of Oncology*, 2010, **2010**, 426218.
178. T. M. Gorges, N. Penkalla, T. Schalk, S. A. Joosse, S. Riethdorf, J. Tucholski, K. Lücke, H. Wikman, S. Jackson, N. Brychta, O. von Ahsen, C. Schumann, T. Krahn and K. Pantel, *Clinical Cancer Research*, 2016, **22**, 2197.
179. C. Chudak, J. Herrmann and T. Lesser, *Journal of Thoracic Oncology*, 2016, **11**, S104-S105.
180. G. Theil, K. Fischer, E. Weber, R. Medek, R. Hoda, K. Lücke and P. Fornara, *PLoS one*, 2016, **11**, e0158354-e0158354.
181. Y. He, J. Shi, G. Shi, X. Xu, Q. Liu, C. Liu, Z. Gao, J. Bai and B. Shan, *Scientific Reports*, 2017, **7**, 9542.
182. D. Mandair, C. Vesely, L. Ensell, H. Lowe, V. Spanswick, J. A. Hartley, M. E. Caplin and T. Meyer, *Endocrine-Related Cancer*, 2016, **23**, L29-L32.
183. O. Vermesh, A. Aalipour, T. J. Ge, Y. Saenz, Y. Guo, I. S. Alam, S.-M. Park, C. N. Adelson, Y. Mitsutake, J. Vilches-Moure, E. Godoy, M. H. Bachmann, C. C. Ooi, J. K. Lyons, K. Mueller, H. Arami, A. Green, E. I. Solomon, S. X. Wang and S. S. Gambhir, *Nature biomedical engineering*, 2018, **2**, 696-705.
184. T. H. Kim, Y. Wang, C. R. Oliver, D. H. Thamm, L. Cooling, C. Paoletti, K. J. Smith, S. Nagrath and D. F. Hayes, *Nature Communications*, 2019, **10**, 1478.
185. J. Xie, Y. Gao, R. Zhao, P. J. Sinko, S. Gu, J. Wang, Y. Li, Y. Lu, S. Yu, L. Wang, S. Chen, J. Shao and L. Jia, *Journal of Controlled Release*, 2015, **209**, 159-169.
186. J. Xie, J. Wang, H. Chen, W. Shen, P. J. Sinko, H. Dong, R. Zhao, Y. Lu, Y. Zhu and L. Jia, *Scientific Reports*, 2015, **5**, 9445.